Function of Nerfin-1 in Preventing Medulla Neurons Dedifferentiation Requires Its Inhibition of Notch Activity

Jiajun Xu[1,5], Xue Hao[1,5], Meng-Xin Yin[1], Yi Lu[1], Yunyun Jin[1], Jinjin Xu[1], Ling Ge[1], Wenqing Wu[1], Margaret Ho[3], Yingzi Yang[4], Yun Zhao[1,2] and Lei Zhang[1,2*]

[1]State Key Laboratory of Cell Biology, CAS Center for Excellence in Molecular Cell Science, Innovation Center for Cell Signaling Network, Institute of Biochemistry and Cell Biology, University of the Chinese Academy of Sciences, Chinese Academy of Sciences, Shanghai 200031, P.R. China.

[2]School of Life Science and Technology, ShanghaiTech University, Shanghai 200031, P.R. China.

[3]Department of Anatomy and Neurobiology, Tongji University, School of Medicine, Shanghai 200092, P.R. China.

[4]Department of Developmental Biology, Harvard School of Dental Medicine, Boston, Massachusetts 02115.

[5]These authors contributed equally to this work.

*Author for correspondence (rayzhang@sibcb.ac.cn).

Keywords: Nerfin-1, medulla neurons, dedifferentiation, Notch signaling

Summary statement

Our findings uncover a novel regulatory mechanism of neuronal maintenance in the optic lobe and reveal the presence of different regulatory modes between the optic lobe and the rest of CNS.

Abstract

Drosophila larval central nervous system comprises the central brain, ventral nerve cord and optic lobe. In these regions, neuroblasts divide asymmetrically to self-renew and generate differentiated neurons or glia. To date, mechanisms of preventing neuron dedifferentiation is still unclear, especially in the optic lobe. Here we show that the zinc finger transcription factor Nerfin-1 is expressed in early stage of medulla neurons and essential for maintaining their differentiation. Loss of Nerfin-1 activates Notch signaling, which promotes neuron-to-NB reversion. Repressing Notch signaling largely rescues dedifferentiation in *nerfin-1* mutant clones. Thus, we conclude that Nerfin-1 represses Notch activity in medulla neurons and prevents them from dedifferentiation.

Introduction

Drosophila larval central nervous system (CNS) comprises central brain (CB), ventral nerve cord (VNC) and optic lobe (OL) (Fig. 1A). Different from the rest of the nervous system developing from neuroectoderm (Hartenstein et al., 2008), *Drosophila* optic lobe originates from a cluster of epithelial cells that invaginate from the posterior procephalic region of the embryonic head (Green et al., 1993). These neuroepithelial (NE) cells, also named the optic lobe placode, develop on both sides of the brain and then grow into the lateral half of the two brain hemispheres at the end of larval development (Green et al., 1993) (Fig. 1A). Later, they give rise to the lamina, medulla, lobula and lobula plate which play important roles in the visual system at adult stage (Fischbach and Dittrich, 1989; Hofbauer and Camposortega, 1990). During development, the optic placode gradually separates into two parts: the inner optic anlagen (IOA) and the outer optic anlagen (OOA) (Green et al., 1993; Hofbauer and Camposortega, 1990; Nassif et al., 2003). At third instar larval stage, NE cells of lateral OOA differentiate into lamina neurons after receiving Hedgehog signals from retinal axons (Huang and Kunes, 1996; Kunes, 2000), while NE cells of medial OOA differentiate into neuroblasts (NBs) under controls of multiple signaling pathways, such as Notch, Hippo, JAK/STAT and EGFR (Egger et al.; Kawamori et al.; Orihara-Ono et al.; Reddy et al.; Yasugi et al.; Yasugi et al., 2008). Such NBs then divide asymmetrically and perpendicularly to the surface, producing a self-renewed NB and a ganglion mother cell (GMC), which further divides into two medulla neurons, pushing the older ones inward (Egger et al., 2007; Nassif et al., 2003; Toriya et al., 2006; Yasugi et al., 2008) (Fig. 1B). Based on these sequential events, it is then possible to judge the age of these neurons by their

spatial location.

In *Drosophila* CNS, the mechanism of medulla neuron dedifferentiation remains unexplored. To date, only Lola, a BTB zinc finger transcription factor, has been reported to maintain the differentiation of medulla neurons in the optic lobe (Southall et al., 2014). Lola functions as a cofactor of Prospero (Pros) and prevents neuron-to-NB reversion by repressing the activity of NB and cell-cycle genes in post-mitotic neurons. Interestingly, loss of Lola induces neuron-to-NB reversion only in medulla neurons, implicating differential mechanisms that inhibit dedifferentiation in the optic lobe and the rest of the CNS. Based on these observations, it is therefore crucial to study the mechanism of medulla neuron dedifferentiation.

Here we show that the zinc finger transcription factor Nervous fingers 1 (Nerfin-1) is expressed in early stage of medulla neurons and essential for maintaining their differentiated state. Loss of Nerfin-1 activates Notch signaling in medulla neurons which promotes neuron dedifferentiation. Inhibition of Notch activity largely blocks dedifferentiation caused by Nerfin-1 depletion and prevents tumourigenesis.

Results

Nerfin-1 is expressed mainly in early stage of medulla neurons

It is known that Hippo pathway plays an important role in the optic lobe (Kawamori et al.; Reddy et al.). Since Nerfin-1 is a possible interacting partner of Hippo effectors Scalloped and Yorkie (Feng et al., 2013; Rhee et al.), we then sought to determine if Nerfin-1 functions in the optic lobe. Throughout the analysis, two cross sections of optic lobe were analyzed (Fig. 1A, C-D'). Layer 1 is the equatorial plane of the brain hemisphere, in which NB lineages are seen distinctively and the order of neuron formation is known by their spatial position. Layer 2 is between the ventral surface and the equatorial plane, in which medulla neurons make up the majority of the optic lobe.

To analyze Nerfin-1 expression pattern, antibodies against Nerfin-1 were generated and used to co-stain the optic lobe with Pros and Embryonic lethal abnormal vision (Elav), which marks the GMC and medulla neurons, respectively. Our results suggested that Nerfin-1 is mainly expressed in differentiated neurons, as its expression overlaps extensively with Elav, but not Pros (Fig. 2A-A'''). This observation was further confirmed using Nerfin-1-GFP flies which express GFP under the *nerfin-1* promoter (Kuzin et al., 2007) (Fig. 2B-B'''). Interestingly, Nerfin-1 protein levels decreased in older neurons, while Nerfin-1-GFP levels remained similar (Fig. 2A'',B''), implicating a post-translational regulation of *nerfin-1* during the development of medulla neurons. Collectively, our results indicate that Nerfin-1 is expressed mainly in the early stage of medulla neurons.

Nerfin-1 absence leads to ectopic NBs in the optic lobe

To examine Nerfin-1 function, flip-out clones expressing Nerfin-1 RNAi transgenes were first generated. Interestingly, large numbers of cells expressed Deadpan (Dpn), a neuroblast marker, despite they were spatially located in where post-mitotic neurons should be (Supplementary Fig. S1A-D). Efficiencies of both Nerfin-1 RNAi lines were confirmed with the Nerfin-1 antibody (Supplemental Fig. S1E-F'). To validate our observation, clones of the null allele *nerfin-1*^{159} were generated using mosaic analysis with a repressible cell marker (MARCM) system (Lee and Luo, 2001) (Supplementary Fig. S1G,G'). Consistent with Nerfin-1 RNAi, a great number of Dpn^{+} cells were detected in *nerfin-1* mutant clones in the medulla cortex (Fig. 3A-C). To determine whether these cells were *bone fide* ectopic NBs, additional NB markers such as Asense (Ase) and Miranda (Mira) were used to examine the optic lobe and similar up-regulation was detected (Fig. 3D-F). Furthermore, these NB-like cells were pH3-positive, exhibited proliferation potential (Fig. 3G-I), and formed brain tumors at adult stage (Fig. 3J). Taken together, we conclude that ectopic NBs are induced in the optic lobe in the absence of Nerfin-1.

Nerfin-1 maintains the differentiation of medulla neurons

To explore the origin of these ectopic NBs, time-course experiments were carried out using the MARCM system. As clones over 24 h always contained multiple NB lineages (Supplementary Fig. S2), quantification could only be done for those within 24 h. In *nerfin-1*^{159} clones within 24 h, only one original NB (Dpn^{+}/Ase^{+}/Mira^{+}) was detected (n>15) (Fig. 4A, Supplementary Fig. S2). Also, Dpn expression was switched off normally in GMCs (Dpn^{-}/Ase^{+}/Mira^{+}) (Fig. 4A) and the number of GMCs remained similar (Fig. 4B).

Furthermore, medulla neurons ($Dpn^-/Ase^-/Mira^-$) were generated normally at 16 h with Ase and Mira expression suppressed (Fig. 4Ad-d'', Supplementary Fig. S2). However, they began to dedifferentiate soon, as weak Dpn staining was detected in several clones (Fig. 4Ae-e''). On the other hand, ectopic Mira and Ase expression appeared 20 h later (Supplementary Fig. S2). Taken together, we conclude that Nerfin-1 absence doesn't affect NB and GMC, thus neurons can be generated, but begin to dedifferentiate at a very early stage. Consistently, Elav was detected in young neurons, but not ectopic Dpn^+ cells generated from dedifferentiation of old neurons (Fig. 4C-D'). Protein level changes in *nerfin-1*^{159} lineages were summarized in Fig. 4E.

To further validate our conclusion, flip-out clones of Nerfin-1 RNAi were induced 96 h after larvae hatched (ALH). Consistent with our expectation, Dpn^+ cells were detected in clones induced in post-mitotic neurons far below the surface (Fig. 4F,F'). Furthermore, *elav-Gal4*, a pan-neuronal Gal4, was used to express Nerfin-1 RNAi in medulla neurons. However, *elav-Gal4* is not strictly expressed in neurons only. Thus, a temperature sensitive Gal80 protein ($Gal80^{ts}$) approach was used to put off the expression. If Nerfin-1 depletion doesn't function in neurons, those generated before Nerfin-1 RNAi misexpression should keep differentiation and ectopic NBs should be found only in superficial layer. Interestingly, ectopic NBs were detected among neurons of different stages (Fig. 4G-I), suggesting that Nerfin-1 is essential for the medulla neurons to maintain their differentiation.

All three zinc fingers contribute to Nerfin-1 function

Nerfin-1 contains three C2H2-type zinc finger domains considered to bind DNA (Supplementary Fig. S3A). To test their function, we generated transgenic flies carrying

Nerfin-1 truncations with single zinc finger deletion (Nerfin-1-dZF1/2/3). As shown in Supplementary Fig. S3B-C'' and G, expression of Nerfin-1 in full length dramatically decreased the number of ectopic NBs in *nerfin-1*^{159} clones. On the other hand, deletion of the first or the second zinc finger alone is sufficient to disrupt Nerfin-1 activity (Supplementary Fig. S3D-E'',G). Nerfin-1-dZF3 only partially inhibited the dedifferentiation (Supplementary Fig. S3F-G). Taken together, all three zinc fingers contribute to Nerfin-1 activity, whereas the first two play a more major role.

Nerfin-1 represses Notch signaling and prevents dedifferentiation

Since Dpn derepression happens earlier than Ase and Mira in *nerfin-1*^{159} clones (Fig. 4A,E, Supplementary Fig. S2), we speculated that mechanisms other than direct transcriptional regulation might be involved. To investigate further, activity of Hippo, JAK/STAT, EGFR and JNK signaling was tested upon losing Nerfin-1. None of these signaling activities were obviously altered (Supplementary Fig. S4). However, Nerfin-1 loss caused dramatic up-regulation of Notch protein level (Fig. 5A,A') and expression of Notch reporters, E(spl)mγ-GFP and Su(H)$_{m8}$-lacZ (Fig. 5B-D), suggesting that Notch pathway might be involved in Nerfin-1-mediated induction of ectopic NBs.

We then analyzed the effect of Notch hyperactivation in the optic lobe. We misexpressed Fringe (Fng), an enhancer of Delta-Notch signaling (Panin et al., 1997), using *elav-Gal4*. As expected, ectopic NBs were detected in medulla cortex (Fig. 5E,F). However, considering the non-specificity of *elav-Gal4* and that Notch signaling promotes NB self-renewal (Bowman et al., 2008; Wang et al., 2006), it is difficult to determine the origin of these ectopic NBs. To confirm the function of Notch hyperactivation in medulla neurons specifically, we

misexpressed Notch intracellular domain (NICD), the constitutively active form of Notch receptor, with *elav-Gal4* and used $Gal80^{ts}$ to control the expression. Consistent with Nerfin-1 RNAi, NICD misexpression induced ectopic NBs among neurons of different stages (Fig. 5G,H). Furthermore, flip-out clones of NICD were induced 96 h ALH. Dpn^{+} cells were found in separate clones induced in post-mitotic neurons far below the surface (Fig. 5I,I'). Same phenotype was detected when the expression of Numb, an inhibitor of Notch signaling, was inhibited (Fig. 5J,J'). Taken together, Notch pathway potentially participates in the dedifferentiation caused by Nerfin-1 absence and promotes the neuron-to-NB reversion.

Inhibition of Notch signaling rescues Nerfin-1-mediated dedifferentiation

Compared with neurons, activity of Notch signaling is higher in NBs (arrowheads, Fig. 5A',B',C'), so it is unclear whether Notch pathway hyperactivation is a cause or a consequence of dedifferentiation. To this end, we knocked down the expression of Notch receptor or Suppressor of Hairless [Su(H)], the transcription factor of Notch pathway (Fortini and Artavanis-Tsakonas, 1994), in the absence of Nerfin-1. As shown in Fig. 6A-H and Supplementary Fig. S5A-D, knockdown of Notch or Su(H) significantly reduced the number of ectopic NBs induced by Nerfin-1 depletion. At the adult stage, Notch knockdown prevented the formation of *nerfin-1*^{159} tumors extensively (Fig. 6I-J'). To confirm these results, we carried out immunostaining analysis and found that up-regulation of Notch receptor and E(spl)mγ-GFP appeared more penetrant than Dpn in *nerfin-1*^{159} clones (Fig. 6K-L'', Supplementary Fig. S5E-E''). These results suggested that hyperactivation of Notch signaling is a cause rather than a consequence of dedifferentiation.

Since Nerfin-1 is mainly expressed in differentiated cells, Notch signaling functions

earlier than Nerfin-1 both spatially and temporally. To this end, we tested if Notch inhibition affects the generation of NB lineage or Nerfin-1 expression. As shown in Fig. 6F', Nerfin-1 exhibited a normal expression level when Notch was knocked down. Next, a time-course experiment was performed (Supplementary Fig. S6A). In Notch RNAi clones within 24 h (n>5 for each), only one original NB was detected and the number of GMC remained similar compared with the control (Supplementary Fig. S6B), indicating that NB lineage is generated normally upon Notch depletion. Taken together, Nerfin-1 loss-of-function induces hyperactivation of Notch signaling which promotes the dedifferentiation of post-mitotic medulla neurons.

Medulla neurons are both the donor and acceptor of Notch signal

To explore whether Notch signaling is constitutively activated when Nerfin-1 is absent, expression of Delta, a ligand of Notch signaling, was knocked down in *nerfin-1*^{159} clones. Interestingly, dedifferentiation caused by Nerfin-1 loss was dramatically suppressed (Fig. 7), indicating that Notch signaling is not constitutively activated, and requires a ligand for its activation. In addition, medulla neurons are both the donor and acceptor of Notch signal.

Medulla neuron dedifferentiation caused by Nerfin-1 loss is independent of dMyc or Tor

A recent study suggests that Nerfin-1 maintains neuron differentiation in both central brains and VNCs (Froldi et al., 2015). In that study, dMyc and Tor were reported to be necessary for the dedifferentiation caused by Nerfin-1 loss. In our present study, however, neither dMyc knockdown nor Tor-DN misexpression inhibited dedifferentiation of medulla neurons in the optic lobe (Supplementary Fig. S7), indicating the presence of differential regulatory mechanisms between the optic lobe and the rest of the CNS.

Discussion

Nerfin-1 exhibits conserved function in maintaining neuron differentiation in *Drosophila* larval CNS

Stem cells generate progeny that undergo terminal differentiation. In *Drosophila* CNS, the balance of self-renewal and differentiation of neural stem and progenitor cells is a central issue during development. On the other hand, the maintenance of differentiated status of post-mitotic neurons is also crucial for tissue function and homeostasis. It is obvious that mechanisms must exist to prevent the cells from dedifferentiation. Although proteins that function to keep differentiation have been well studied in other cell types (Bello et al., 2006; Betschinger et al., 2006; Eroglu et al.; Koe et al., 2014; Lee et al., 2006; Wang et al., 2007; Weng et al.; Zhang et al., 2016), few have been implicated in post-mitotic neuronal maintenance. In the central brain, loss of Midlife crisis (Mdlc), a CCCH-zinc finger protein, results in a decrease of Pros, thus derepressing NB genes in neurons (Carney et al., 2013). However, it is insufficient to make neurons revert to proliferating NBs. Furthermore, since Pros is not expressed in medulla neurons, it is unclear if Mdlc has the same function in the optic lobe. On the other hand, Lola absence leads to neuron-to-NB reversion and tumourigenesis (Southall et al., 2014), but it is crucial for neuronal maintenance only in the optic lobe. Recently, a paper reported that Nerfin-1 loss induces neuron dedifferentiation in both central brain and VNC (Froldi et al., 2015). In the present study, we demonstrate a conserved function of Nerfin-1 in medulla neurons in the optic lobe. Our findings indicate that Nerfin-1 is expressed in the early stage of medulla neurons and functions to maintain their differentiated state.

Differential mechanisms of neuronal maintenance between the optic lobe and the rest of the CNS

Interestingly, we noticed that ectopic NB induced by Nerfin-1 depletion in the optic lobe appeared much earlier than that in the central brain. Considering that Lola loss causes dedifferentiation just in the optic lobe (Southall et al., 2014), we speculate that the differentiated state of medulla neurons is less stable, possibly due to Pros absence. Furthermore, different from the mechanism in the central brain, function of Nerfin-1 in the optic lobe requires a silence of Notch signaling. Neither dMyc knockdown nor Tor-DN misexpression inhibits dedifferentiation caused by Nerfin-1 loss in the medulla neurons (Supplementary Fig. S7). Thus, our findings identify a distinct regulatory mechanism in medulla neurons and validate different regulatory modes between the optic lobe and the rest of the CNS.

Cyclin E expression is not affected directly by Nerfin-1 to maintain medulla neuron differentiation

On the other hand, cell cycle genes play important roles in cell differentiation. Among them, Cyclin E (CycE) is reported to be regulated directly by Lola-N (Southall et al., 2014) and involved in the neuron dedifferentiation caused by loss of Midlife crisis (Mdlc) (Carney et al., 2013). Thus, we also examined whether CycE is regulated directly by Nerfin-1 and controls cell differentiation independently of Notch and neuroblast genes. Interestingly, CycE expression levels were up-regulated dramatically in *nerfin-1*^{159} clones, but such up-regulation was mostly blocked by Notch repression (data not shown). These results suggest that CycE is not a direct target of Nerfin-1 to maintain medulla neuron differentiation. CycE acts

downstream of Notch signaling or it is subsequently up-regulated after cell type change.

Notch signaling is inhibited by a suppression of Notch receptor expression

Since Notch signaling is hyper activated in *nerfin-1* mutant clones, we are interested in how it is regulated. One possibility is that Notch signaling becomes constitutively activated without the inhibition by Nerfin-1. To this end, we knocked down Delta upon Nerfin-1 loss and found dedifferentiation suppressed (Fig. 7). These results indicate that Notch signaling is not constitutively activated, and needs a ligand. What's more, Notch signal is both produced and received by medulla neurons. At the same time, our results have showed that Nerfin-1 loss induces dramatic up-regulation on the expression level of Notch receptor (Fig. 5A,A'). Thus, we hypothesize that Nerfin-1 suppresses the expression of Notch receptor in normal medulla neurons and inhibits Notch pathway activity. When Nerfin-1 is absent, expression level of Notch receptor increases strikingly. The receptors then bind to Delta from the adjacent cells and activate Notch signaling in its own. However, it is still unclear whether Notch receptor is a direct target of Nerfin-1. Therefore, subsequent studies on Nerfin-1 may help us to clarify the underlying mechanisms and provide better understanding about neuronal maintenance.

Materials and Methods

Fly strains

Flies were raised on standard yeast/molasses medium at 25°C unless otherwise stated.

The full length Nerfin-1 DNA fragment (1410 bp) was amplified from *Drosophila* cDNA. Nerfin-1-dZF1/ 2/ 3 are truncations of Nerfin-1 with 748-810 bp/ 832-900 bp/ 1000-1068 bp deleted respectively. Fragments were inserted into *pUAST-attb* vector and verified by DNA sequencing. Nerfin-1 full length and dZF1/ 2/ 3 transgenic flies were generated by site-specific integration into the fly genome at 25C6 attp locus.

Ectopic expression clones were created by Flip-out using:

hsflp[122] act>CD2>Gal4; UAS-Dicer2 UAS-GFP (referred as AG4),

Nerfin-1 RNAi-1 (VDRC #101631),

Nerfin-1 RNAi-2 (Bloomington #28324),

yw;; HA-NICD (Han et al., 2016),

Numb RNAi (Bloomington #35045),

dMyc RNAi (VDRC #106066),

Su(H) RNAi (Bloomington #28900),

Mutant clones were created by FLP-FRT-mediated recombination using:

hsflp[122]; tub-Gal4 UAS-GFP; FRT80 tub-Gal80,

hsflp[122];; FRT80,

Df(3L)FRT80 nerfin-1^{159}*/TM6B* (gift from W. F. Odenwald) (Kuzin et al., 2005),

Markers of gene expression and activity:

ex-lacZ (Hamaratoglu et al., 2006),

puc-lacZ (*puc*^{E69}, DGRC #109029),

Su(H)$_{m8}$*-lacZ* (gift from Rongwen Xi and Sarah Bray) (Furriols and Bray, 2001; Lin et al., 2010),

E(spl)m γ-GFP (gift from Hongyan Wang),

Other drivers and fly strains:

elav-Gal4[C155] (Lin and Goodman, 1994),

elav-Gal4[C155];; tubGal80^{ts},

P[nerfin-1.GFP-NLS.SV-40] iA (referred as Ner-1-GFP, gift from A. Kuzin) (Kuzin et al., 2007),

UAS-Tor-DN (Bloomington #7013),

Notch RNAi (VDRC #100002),

Delta RNAi (VDRC #36784),

w; UAS-Fng (Bloomington #8553),

UAS-Dicer2.

Immunostaining

Tissues were dissected in PBS and fixed in 4% formaldehyde in PBS for 15-20 min at room temperature. Wash solution was PBS with 0.1% (larval tissues) or 0.3% (adult brains) Triton X-100.

Primary antibodies used in this study: mouse anti Pros (1:100, DSHB), rabbit anti Dpn (1:200, gift from Hongyan Wang), guinea pig anti Dpn (1:1000, gift from Xiaohang Yang), rat anti Elav (1:100, DSHB), rabbit anti Nerfin-1 (1:100), mouse anti Mira (1:50, gift from Hongyan Wang), guinea pig anti Ase (1:500, gift from Hongyan Wang), rabbit anti pH3

(1:100, Millipore), mouse anti NICD (1:100, DSHB), rabbit anti lacZ (1:500, Invitrogen), rabbit anti pSTAT (1:500, gift from Xinhua Lin), rabbit anti pErk (1:100, Cell signaling), rabbit anti dMyc (1:100, Santa Cruz Biotechnology). F-actin was stained with phalloidin (1:20000, Thermo Fisher Scientific) together with the secondary antibodies. Rabbit anti Nerfin-1 (1-240aa) was made by ABclonal. Secondary goat or donkey antibodies (Jackson) were used at 1:1500. Samples were mounted with Vectashield mounting media (Vector Laboratories).

Clonal analysis and temperature shift experiments

To induce flip-out clones, larvae were heat shocked 24 h ALH for 15 min at 37°C and dissected 96 h later unless otherwise stated. To induce NICD clones, larvae were heat shocked 96 h ALH for 7 min at 37°C and dissected 24 h later.

To induce *nerfin-1*^{159} clones, larvae were heat shocked 24 h ALH for 30 min at 37°C and dissected 96 h later unless otherwise stated. For time-course assay, embryos were collected for 4 h. Larvae were heat shocked 108/104/96/84/72/60 h ALH and dissected 120 h ALH. MARCM clones in the adult brains were induced by heat shocking larvae 24 h ALH for 30 min at 37°C and flies were dissected 7 days after eclosion.

Gal80^{ts} is a temperature sensitive Gal80 protein which is functional at 18℃ and non-functional at 29℃. To put off the expression of transgenes, larvae were raised at 18℃ for 9-10 days and then transferred to 29℃. Dissection was done 24 h later.

Microscopy image acquisition and Statistics

Fluorescent microscopy was performed on a Leica LAS SP8 confocal microscope; confocal images were obtained using the Leica AF Lite system. Larval tissues were taken

photos using a 40× objective and adult brains were using a 20× objective. All the data were expressed as the mean standard error of the mean (SEM) and were analyzed using Student's t-test. The results were considered statistically significant if $p<0.05$.

To quantify the expression of $Su(H)_{m8}$-lacZ in figure. 5C, intensity of the lacZ and GFP signal in the thick dash line region was analyzed using the Leica AF Lite system. 210 pixels were analyzed, in which 124 (GFP^-) were quantified as *WT* while 86 (GFP^+) were *nerfin-1*^{159}.

Acknowledgements

We would like to thank Hongyan Wang, W. F. Odenwald, A. Kuzin, Louise Y. Cheng, Rongwen Xi, Lei Xue, Xinhua Lin, Renjie Jiao, Xiaohang Yang, Sarah Bray, Zhangwu Zhao, Shigeo Hayashi, Wu-Min Deng, Shian Wu, Stephen Crews, André Bachmann, the Bloomington Drosophila center, National institute of Genetics, Vienna Drosophila RNAi Centers, Kyoto Stock Center (DGRC) and the Developmental Studies Hybridoma Bank for reagents and fly stocks.

Competing interests

The authors declare no conflict of interest.

Author contributions

J.X. and L.Z. conceived and designed the experiments; J.X., X.H., Y.L., Y.J., J.X. performed the experiments; J.X., X.H., L.Z. analyzed the data; L.G., W.W., Y.Z. contributed regents/materials; J.X., M.Y., M.H.,Y.Y., L.Z. wrote and edited the paper.

Funding

This research is supported by the Strategic Priority Research Program of the Chinese Academy of Sciences (XDB19000000), the National Natural Science Foundation of China (31625017, 31530043, 31371462), the “Cross and cooperation in science and technology innovation team” project of the Chinese Academy of Sciences, and the CAS/SAFEA International Partnership Program for Creative Research Teams.

References

Bello, B., Reichert, H. and Hirth, F. (2006). The brain tumor gene negatively regulates neural progenitor cell proliferation in the larval central brain of Drosophila. *Development* **133**, 2639-2648.

Betschinger, J., Mechtler, K. and Knoblich, J. A. (2006). Asymmetric Segregation of the Tumor Suppressor Brat Regulates Self-Renewal in Drosophila Neural Stem Cells. *Cell* **124**, 1241-1253.

Bowman, S. K., Rolland, V., Betschinger, J., Kinsey, K. A., Emery, G. and Knoblich, J. A. (2008). The tumor suppressors Brat and Numb regulate transit-amplifying neuroblast lineages in Drosophila. *Dev Cell* **14**, 535-546.

Carney, T. D., Struck, A. J. and Doe, C. Q. (2013). midlife crisis encodes a conserved zinc-finger protein required to maintain neuronal differentiation in Drosophila. *Development* **140**, 4155-4164.

Egger, B., Boone, J. Q., Stevens, N. R., Brand, A. H. and Doe, C. Q. (2007). Regulation of spindle orientation and neural stem cell fate in the Drosophila optic lobe. *Neural Dev* **2**, 1.

Egger, B., Gold, K. S. and Brand, A. H. Notch regulates the switch from symmetric to asymmetric neural stem cell division in the Drosophila optic lobe. *Development* **137**, 2981-2987.

Eroglu, E., Burkard, T. R., Jiang, Y., Saini, N., Homem, C. C., Reichert, H. and Knoblich, J. A. SWI/SNF Complex Prevents Lineage Reversion and Induces Temporal Patterning in Neural Stem Cells. *Cell* **156**, 1259-1273.

Feng, G., Yi, P., Yang, Y., Chai, Y., Tian, D., Zhu, Z., Liu, J., Zhou, F., Cheng, Z., Wang, X., et al. (2013). Developmental stage-dependent transcriptional regulatory pathways control neuroblast lineage progression. *Development* **140**, 3838-3847.

Fischbach, K.-F. and Dittrich, A. (1989). The optic lobe of Drosophila melanogaster. I. A Golgi analysis of wild-type structure. *Cell and tissue research* **258**, 441-475.

Fortini, M. E. and Artavanis-Tsakonas, S. (1994). The suppressor of hairless protein participates in notch receptor signaling. *Cell* **79**, 273-282.

Froldi, F., Szuperak, M., Weng, C. F., Shi, W., Papenfuss, A. T. and Cheng, L. Y. (2015). The transcription factor Nerfin-1 prevents reversion of neurons into neural stem cells. *Genes Dev* **29**, 129-143.

Furriols, M. and Bray, S. (2001). A model Notch response element detects Suppressor of Hairless-dependent molecular switch. *Curr Biol* **11**, 60-64.

Green, P., Hartenstein, A. Y. and Hartenstein, V. (1993). The embryonic development of the Drosophila visual system. *Cell Tissue Res* **273**, 583-598.

Hamaratoglu, F., Willecke, M., Kango-Singh, M., Nolo, R., Hyun, E., Tao, C., Jafar-Nejad, H. and Halder, G. (2006). The tumour-suppressor genes NF2/Merlin and Expanded act through Hippo signalling to regulate cell proliferation and apoptosis. *Nat Cell Biol* **8**, 27-36.

Han, H., Fan, J., Xiong, Y., Wu, W., Lu, Y., Zhang, L. and Zhao, Y. (2016). Chi and dLMO function antagonistically on Notch signaling through directly regulation of fng transcription. *Scientific reports* **6**, 18937.

Hartenstein, V., Spindler, S., Pereanu, W. and Fung, S. (2008). The development of the Drosophila larval brain. *Adv Exp Med Biol* **628**, 1-31.

Hofbauer, A. and Camposortega, J. A. (1990). Proliferation Pattern and Early Differentiation of the Optic Lobes in Drosophila-Melanogaster. *Roux Arch Dev Biol* **198**, 264-274.

Huang, Z. and Kunes, S. (1996). Hedgehog, transmitted along retinal axons, triggers neurogenesis in the developing visual centers of the Drosophila brain. *Cell* **86**, 411-422.

Kawamori, H., Tai, M., Sato, M., Yasugi, T. and Tabata, T. Fat/Hippo pathway regulates the progress of neural differentiation signaling in the Drosophila optic lobe. *Dev Growth Differ* **53**, 653-667.

Koe, C. T., Li, S., Rossi, F., Wong, J. J., Wang, Y., Zhang, Z., Chen, K., Aw, S. S., Richardson, H. E., Robson, P., et al. (2014). The Brm-HDAC3-Erm repressor complex suppresses dedifferentiation in Drosophila type II neuroblast lineages. *eLife* **3**, e01906.

Kunes, S. (2000). Axonal signals in the assembly of neural circuitry. *Curr Opin Neurobiol* **10**, 58-62.

Kuzin, A., Brody, T., Moore, A. W. and Odenwald, W. F. (2005). Nerfin-1 is required for early axon guidance decisions in the developing Drosophila CNS. *Dev Biol* **277**, 347-365.

Kuzin, A., Kundu, M., Brody, T. and Odenwald, W. F. (2007). The Drosophila nerfin-1 mRNA requires multiple microRNAs to regulate its spatial and temporal translation dynamics in the developing nervous system. *Dev Biol* **310**, 35-43.

Lee, C. Y., Wilkinson, B. D., Siegrist, S. E., Wharton, R. P. and Doe, C. Q. (2006). Brat is a Miranda cargo protein that promotes neuronal differentiation and inhibits neuroblast self-renewal. *Dev Cell* **10**, 441-449.

Lee, T. and Luo, L. (2001). Mosaic analysis with a repressible cell marker (MARCM) for Drosophila neural development. *Trends in neurosciences* **24**, 251-254.

Lin, D. M. and Goodman, C. S. (1994). Ectopic and increased expression of Fasciclin II alters motoneuron growth cone guidance. *Neuron* **13**, 507-523.

Lin, G., Xu, N. and Xi, R. (2010). Paracrine unpaired signaling through the JAK/STAT pathway controls self-renewal and lineage differentiation of drosophila intestinal stem cells. *Journal of molecular cell biology* **2**, 37-49.

Nassif, C., Noveen, A. and Hartenstein, V. (2003). Early development of the Drosophila brain: III. The pattern of neuropile founder tracts during the larval period. *The Journal of comparative neurology* **455**, 417-434.

Orihara-Ono, M., Toriya, M., Nakao, K. and Okano, H. Downregulation of Notch mediates the seamless transition of individual Drosophila neuroepithelial progenitors into optic medullar neuroblasts during prolonged G1. *Dev Biol* **351**, 163-175.

Panin, V. M., Papayannopoulos, V., Wilson, R. and Irvine, K. D. (1997). Fringe modulates Notch-ligand interactions. *Nature* **387**, 908-912.

Reddy, B. V., Rauskolb, C. and Irvine, K. D. Influence of fat-hippo and notch signaling on the proliferation and differentiation of Drosophila optic neuroepithelia. *Development* **137**, 2397-2408.

Rhee, D. Y., Cho, D. Y., Zhai, B., Slattery, M., Ma, L., Mintseris, J., Wong, C. Y., White, K. P., Celniker, S. E., Przytycka, T. M., et al. Transcription factor networks in Drosophila melanogaster. *Cell Rep* **8**, 2031-2043.

Southall, T. D., Davidson, C. M., Miller, C., Carr, A. and Brand, A. H. (2014). Dedifferentiation of neurons precedes tumor formation in Lola mutants. *Dev Cell* **28**, 685-696.

Toriya, M., Tokunaga, A., Sawamoto, K., Nakao, K. and Okano, H. (2006). Distinct functions of human numb isoforms revealed by misexpression in the neural stem cell lineage in the Drosophila larval brain. *Developmental neuroscience* **28**, 142-155.

Wang, H., Ouyang, Y., Somers, W. G., Chia, W. and Lu, B. (2007). Polo inhibits progenitor self-renewal and regulates Numb asymmetry by phosphorylating Pon. *Nature* **449**, 96-100.

Wang, H., Somers, G. W., Bashirullah, A., Heberlein, U., Yu, F. and Chia, W. (2006). Aurora-A acts as a tumor suppressor and regulates self-renewal of Drosophila neuroblasts. *Genes Dev* **20**, 3453-3463.

Weng, M., Golden, K. L. and Lee, C. Y. dFezf/Earmuff maintains the restricted developmental potential of intermediate neural progenitors in Drosophila. *Dev Cell* **18**, 126-135.

Yasugi, T., Sugie, A., Umetsu, D. and Tabata, T. Coordinated sequential action of EGFR and Notch signaling pathways regulates proneural wave progression in the Drosophila optic lobe. *Development* **137**, 3193-3203.

Yasugi, T., Umetsu, D., Murakami, S., Sato, M. and Tabata, T. (2008). Drosophila optic lobe neuroblasts triggered by a wave of proneural gene expression that is negatively regulated by JAK/STAT. *Development* **135**, 1471-1480.

Zhang, Y., Rai, M., Wang, C., Gonzalez, C. and Wang, H. (2016). Prefoldin and Pins synergistically regulate asymmetric division and suppress dedifferentiation. *Scientific reports* **6**, 23735.

Figures

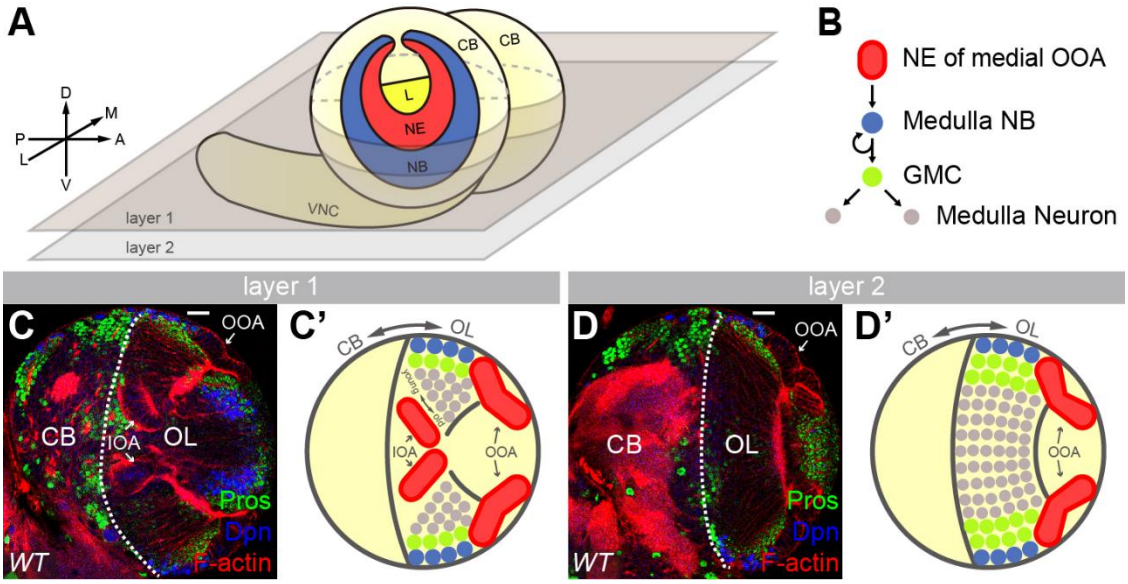

Figure. 1 *Drosophila* larval optic lobe anatomy. (A) Schematic of larval CNS. NE cells (red), medulla NBs (blue) and lamina (L, yellow) in the optic lobe are shown. The gray planes show the cross sections scanned in this study. CB, central brain; VNC, ventral nerve cord. (B) Schematic depicting neurogenesis in medulla cortex. (C-D') Confocal (C,D) and schematics (C',D') of two cross sections of larval brain correspond to layer 1 (C,C') and layer 2 (D,D') respectively in (A). Dash lines represent the CB-OL boundary. Dpn marks neuroblast and F-actin draws the outline. OL, optic lobe; IOA, inner optic anlagen; OOA, outer optic anlagen.

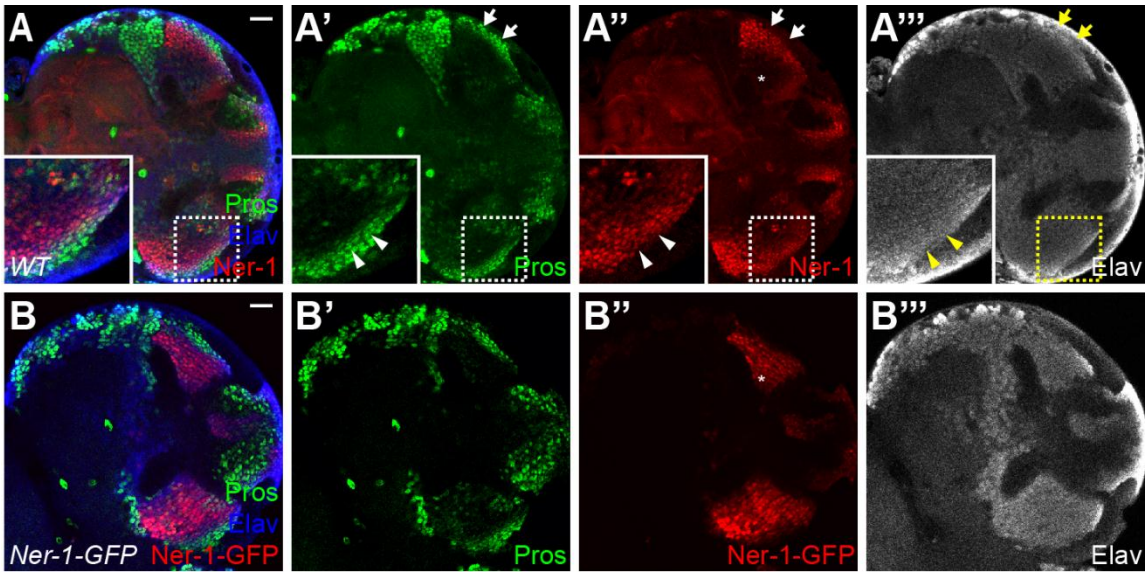

Figure. 2 *nerfin-1* expression in medulla neurons. (A-A''') Representative larval brains showing Nerfin-1, Pros and Elav staining. Insets are magnification of boxed regions. Arrowheads and arrows mark the edge of neurons and GMCs respectively. Asterisk in A'' marks Nerfin-1^{-} old neurons. (B-B''') Representative larval brains showing Nerfin-1-GFP, Pros and Elav staining. Asterisk in B'' marks Nerfin-1-GFP^{+} old neurons. Scale bars represent 20 μm.

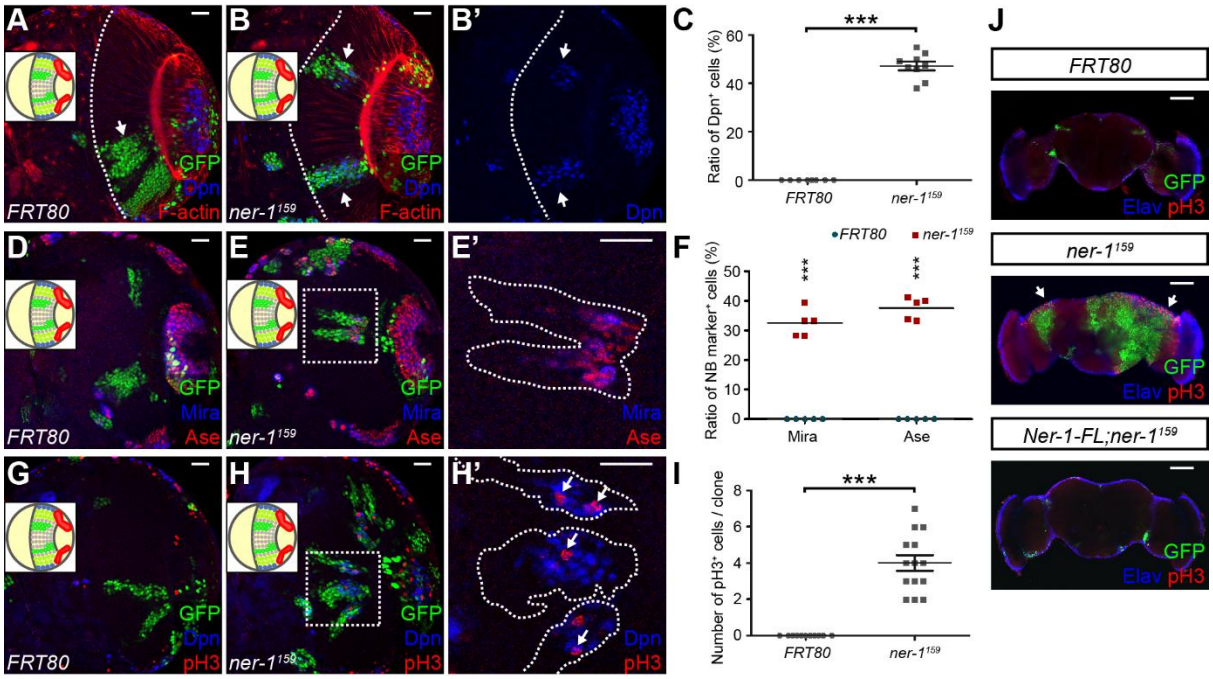

Figure. 3 Nerfin-1 depletion results in ectopic NBs and tumorigenesis. (A-B') Nerfin-1 depletion induces ectopic Dpn$^+$ cells in the medulla cortex. Arrows show the clones. Dash lines represent the CB-OL boundary. Insets show clone regions schematically. (C) Quantification of the ratio of Dpn$^+$ cells in clones from (A,B). n=8,9, respectively. Mean±SEM; *** p<0.001. (D-E') Nerfin-1 depletion induces ectopic Mira$^+$ and Ase$^+$ cells in the medulla cortex. Insets show clone regions schematically. (E') is the magnification of boxed region in (E) with clone outlined. (F) Quantification of the ratio of Mira$^+$ or Ase$^+$ cells in clones from (D,E). n=5 for each. Mean±SEM; *** p<0.001. (G-H') Ectopic Dpn$^+$ cells are able to proliferate. pH3 labels cells undergoing mitosis. Insets show clone regions schematically. (H') is the magnification of boxed region in (H) with clones outlined. Arrows mark pH3$^+$/Dpn$^+$ cells. (I) Quantification of the number of pH3$^+$ cells in clones from (G,H).

n=11,14, respectively. Mean±SEM; *** $p<0.001$. (J) Nerfin-1 depletion induces tumors in adult brain which is rescued by expression of Nerfin-1 full length. Arrows mark the tumors. Scale bars represent 100 μm in (J) and 20μm for the rest.

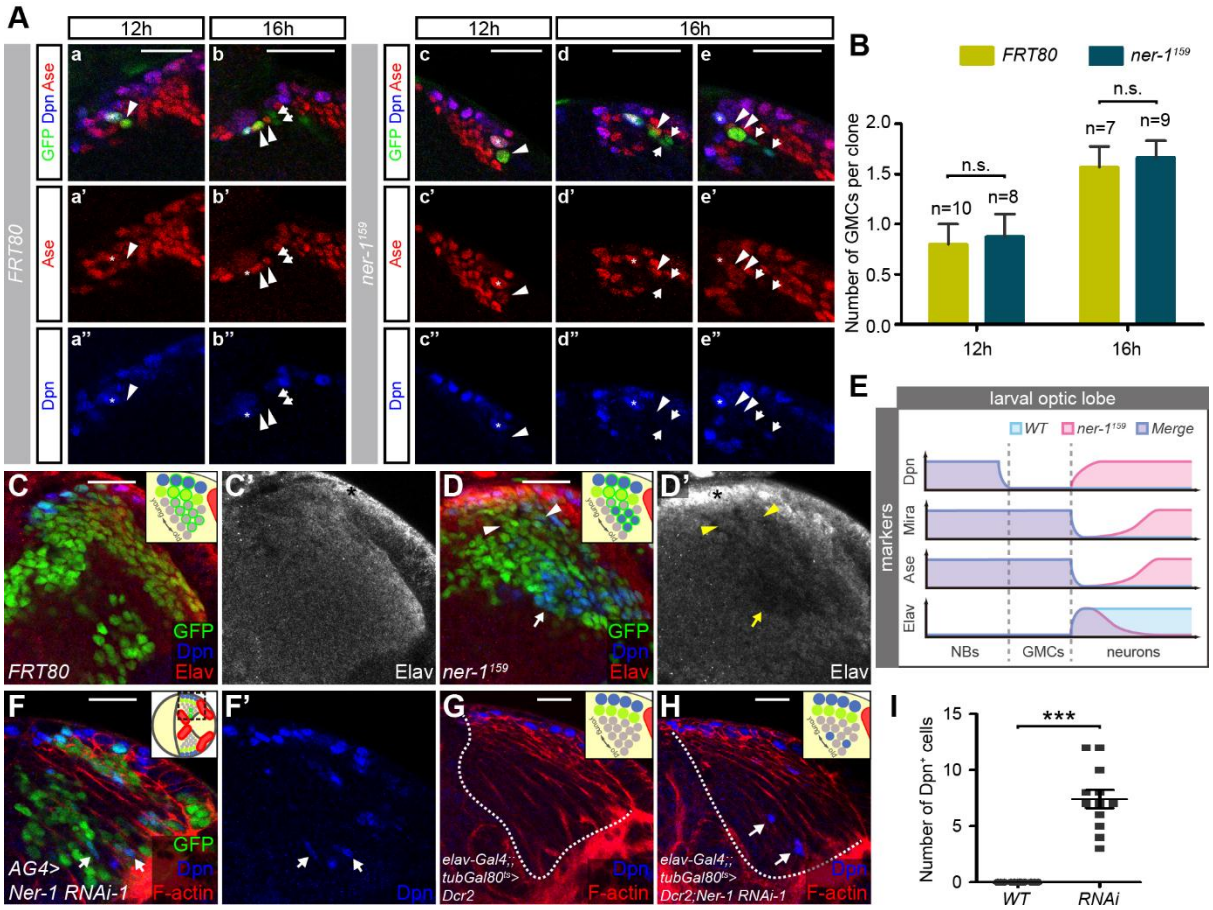

Figure. 4 Nerfin-1 absence results in dedifferentiation of medulla neurons. (A) Time-course experiment of control and *nerfin-1*^{159}. Representative NB lineages labeled by GFP were shown. NB, GMC and neuron are marked by asterisk, arrowhead and arrow respectively. (B) Quantification of the number of GMCs in clones from (A). Mean±SEM; n.s. no significant. (C-D') Representative clones of control (C,C') and *nerfin-1*^{159} (D,D'), showing Dpn and Elav staining. Asterisk marks unspecific signals of Elav antibody. Arrow marks Elav^{-} cells. Arrowheads mark Elav^{+} cells. Insets show clone regions schematically. (E) Schematic diagram showing the temporal expression of Dpn, Mira, Ase and Elav during

medulla neuronal differentiation. (F,F') Ectopic NBs are detected in flip-out clones of Nerfin-1 RNAi. Dicer2 (Dcr2) is used to enhance the function of RNAi. Arrows mark the clones. Insets show clone regions schematically. (G,H) Nerfin-1 knockdown leads to ectopic NBs in the medulla cortex. Dash lines represent the CB-OL boundary. Insets show clone regions schematically. Arrows in (H) show ectopic NBs among neurons of late stage. (I) Quantification of the number of Dpn^+ cells according to (G,H). n=12 for each. Mean±SEM; *** $p<0.001$. Scale bars represent 20 μm.

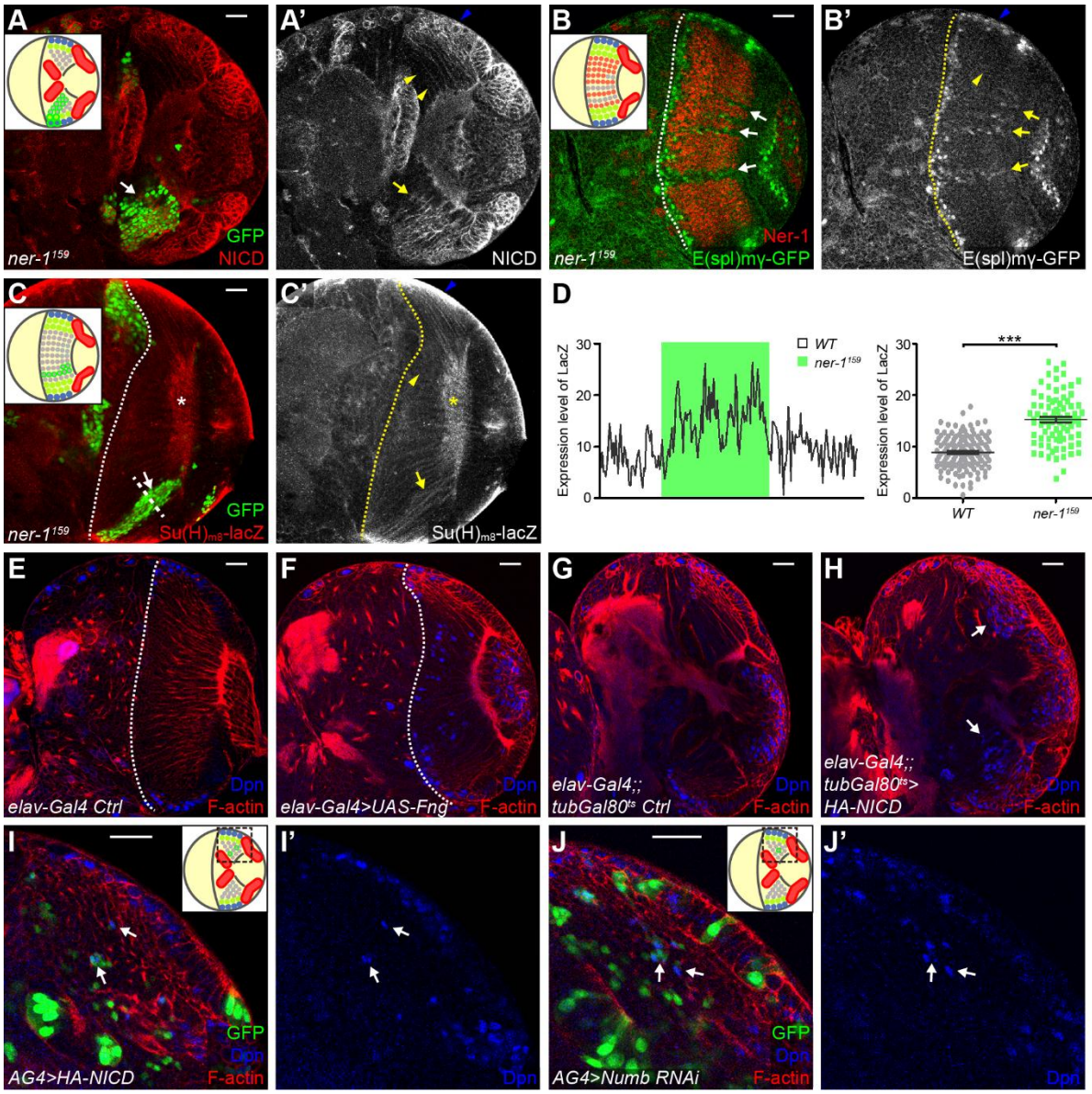

Figure. 5 Notch activity is up-regulated in *nerfin-1*^{159} clones and hyperactivation of Notch signaling leads to ectopic NBs. (A-C') Expression level of Notch receptor (A,A'), E(spl)mγ-GFP (B,B') and Su(H)$_{m8}$-lacZ (C,C') is up-regulated in *nerfin-1*^{159} clones. Arrows mark *nerfin-1*^{159} clones. Blue and yellow arrowheads mark normal NBs and neurons respectively. Dash lines represent the CB-OL boundary. Insets show clone regions

schematically. Clones in (B) are labeled by loss of Nerfin-1. Asterisks in (C,C') mark unspecific signals of lacZ antibody. (D) Quantification of lacZ expression in the region marked by thick dash line in (C). Mean±SEM; *** $p<0.001$. (E-H) Misexpression of Fringe (E,F) and NICD (G,H) leads to ectopic NBs in the medulla cortex. Dash lines represent the CB-OL boundary. Arrows in (H) show ectopic NBs among neurons of late stage. (I-J') Ectopic NBs are detected in flip-out clones of NICD (I,I') and Numb RNAi (J,J'). Clones were induced 96 h ALH. Arrows mark the clones. Insets show clone regions schematically. Scale bars represent 20 μm.

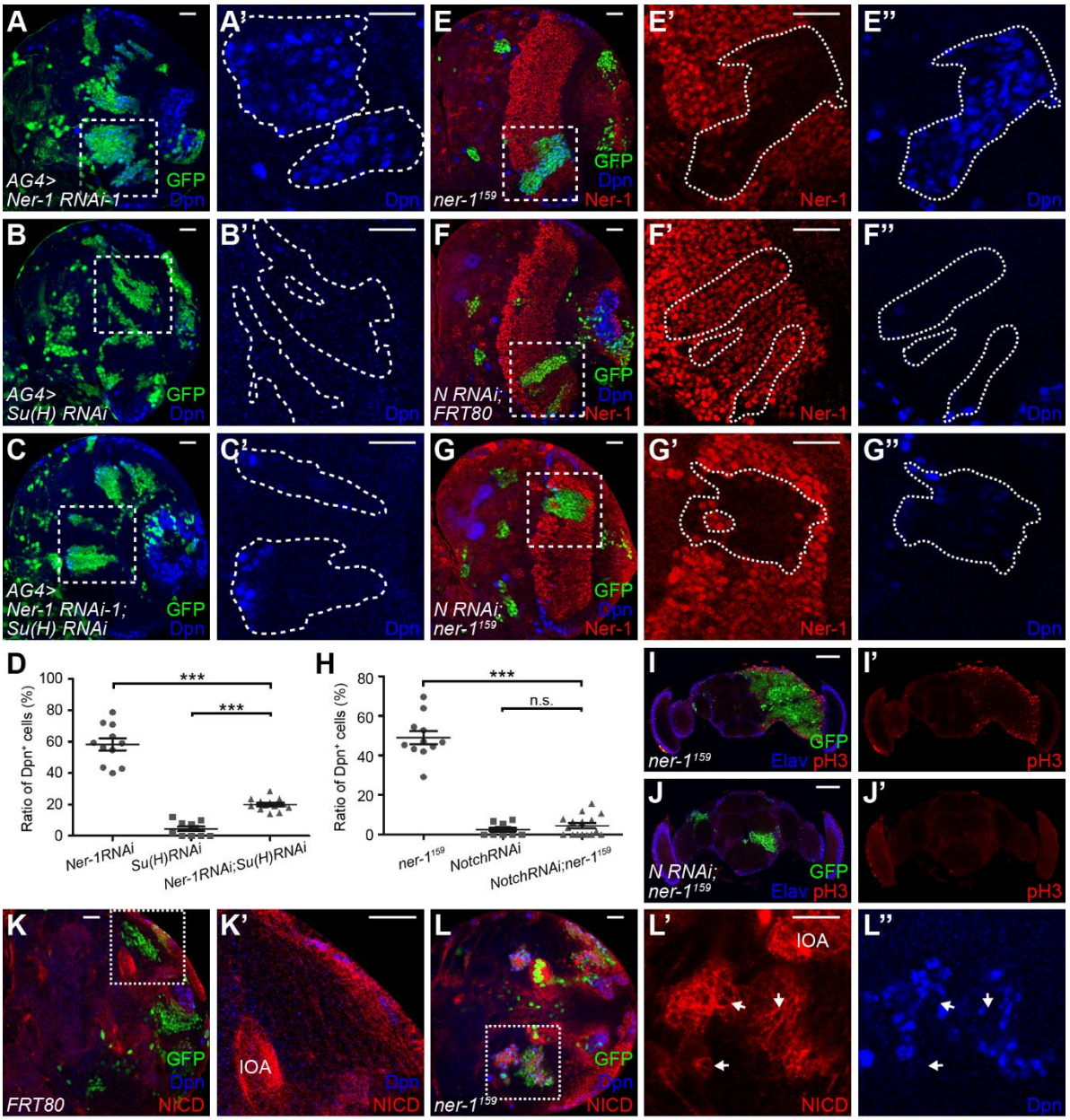

Figure. 6 Dedifferentiation caused by Nerfin-1 depletion is rescued by repression of Notch signaling. (A-C') Knockdown of Su(H) significantly reduces Dpn$^+$ cells in Nerfin-1 RNAi clones. Magnification of boxed regions in (A,B,C) is shown in (A',B',C') respectively with clones outlined. (D) Quantification of the ratio of Dpn$^+$ cells in clones from (A,B,C).

n=11,10,13, respectively. Mean±SEM; *** p<0.001. (E-G'') Notch Knockdown doesn't affect Nerfin-1 expression but reduces the number of Dpn^+ cells in *nerfin-1*^{159} clones. Magnification of boxed regions in (E,F,G) is shown in (E'-G'') with clones outlined. (H) Quantification of the ratio of Dpn^+ cells in clones from (E,F,G). n=11,10,16, respectively. Mean±SEM; n.s. no significant; *** p<0.001. (I-J') Notch Knockdown significantly rescues *nerfin-1*^{159} tumors at adult stage. (K-L'') Up-regulation of Notch expression is more extensive than Dpn in *nerfin-1*^{159} clones. Magnification of boxed region in (K) and (L) is shown in (K') and (L',L'') respectively. Arrows mark the $NICD^+/Dpn^-$ cells. Scale bars represent 100 μm in (I,J) and 20μm for the rest.

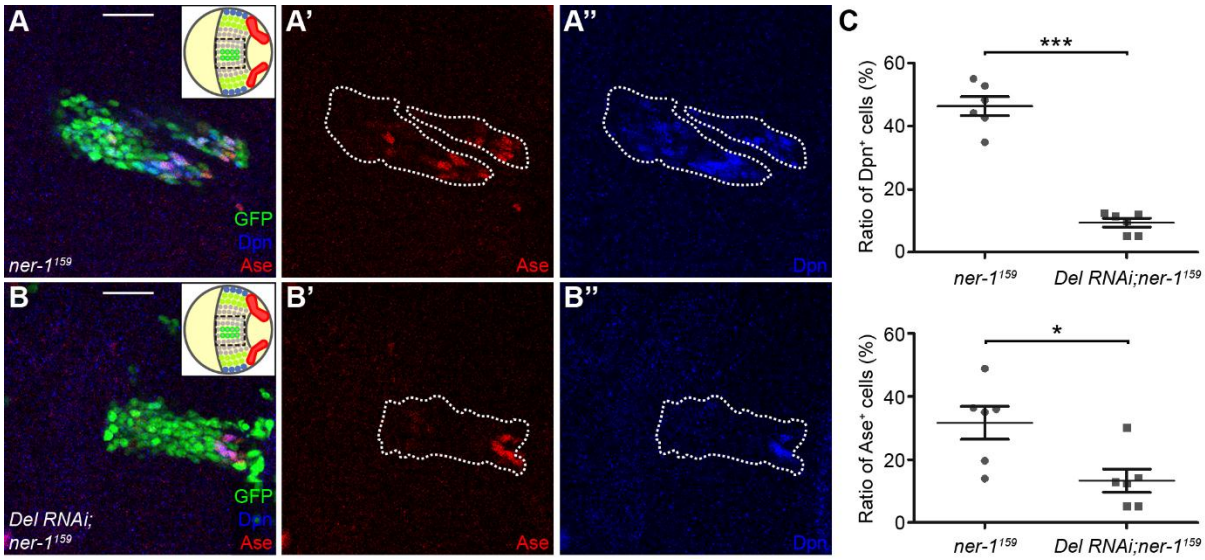

Figure. 7 Dedifferentiation caused by Nerfin-1 absence is suppressed by Delta knockdown. (A-B'') Representative *nerfin-1*^{159} clones with and without Delta RNAi showing Dpn and Ase staining. Insets show clone regions schematically. Dash lines outline the clone region. Scale bars represent 20 μm. (C) Quantification of the ratio of Dpn^{+} or Ase^{+} cells in clones from (A,B). n=6 for each. Mean±SEM; * $p<0.05$; *** $p<0.001$.

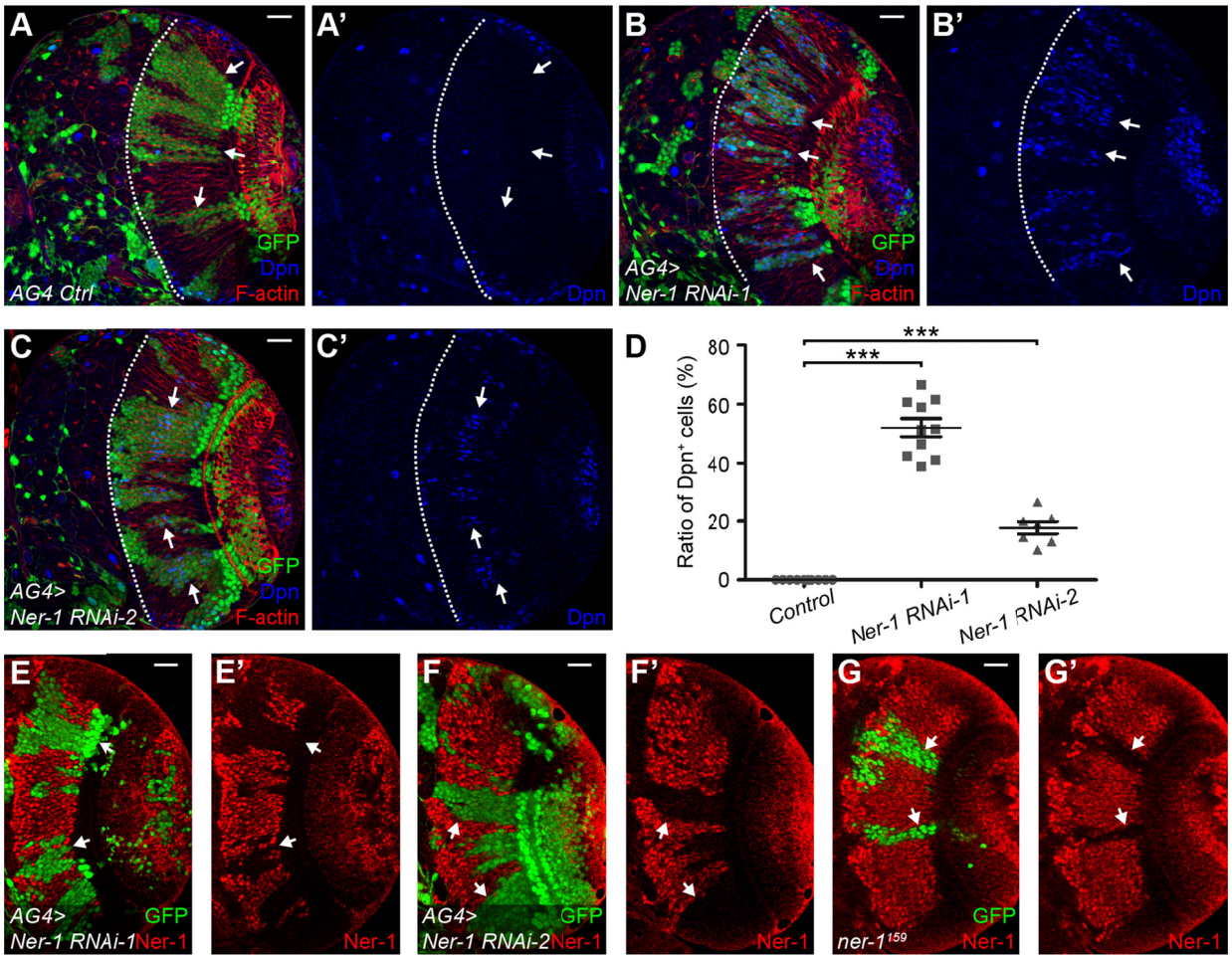

Figure. S1 Nerfin-1 knockdown results in ectopic NBs in medulla cortex.

(A-C') Knockdown of Nerfin-1 induces ectopic Dpn$^+$ cells. Arrows mark the clones. Dash lines represent the boundary between central brain and the optic lobe. (D) Quantification of the number of Dpn$^+$ cells in clones from (A,B,C). n=10,10,7, respectively. Mean ± SEM; *** p<0.001. (E-G') Confirmation of the efficiency of Nerfin-1 RNAi lines (E-F') or *nerfin-1*^{159} fly (G,G'). Arrows mark the clones. Scale bars represent 20 μm. Clones are all labeled by GFP.

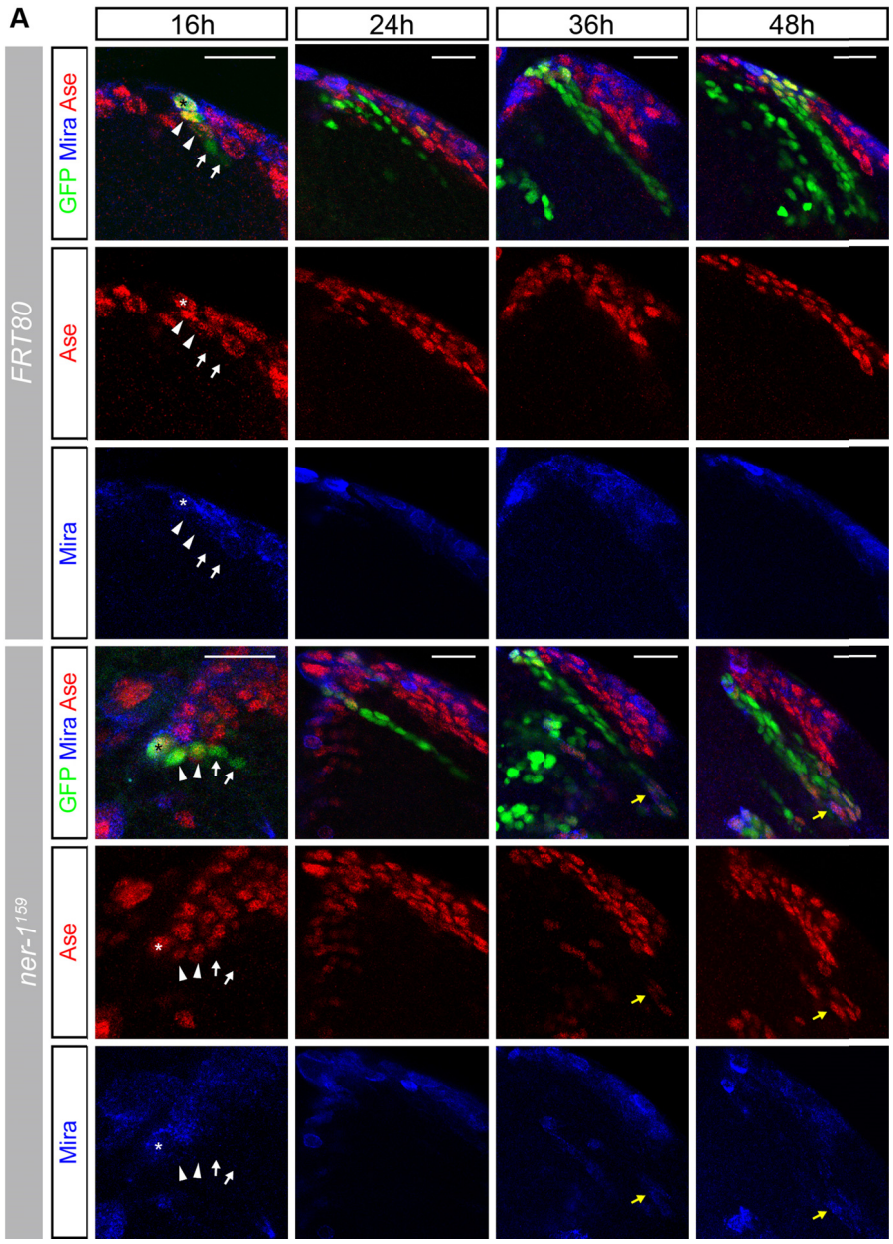

Figure. S2 Nerfin-1 loss leads to ectopic expression of Mira and Ase.

(A) Time-course experiment showing Mira and Ase staining. Representative clones of NB lineages labeled by GFP are shown. Asterisk, arrowhead and arrow mark NB, GMC and neuron respectively in clones of 16 h. Yellow arrows show ectopic expression of Mira and Ase in *nerfin-1*^{159} clones. Scale bars represent 20 μm.

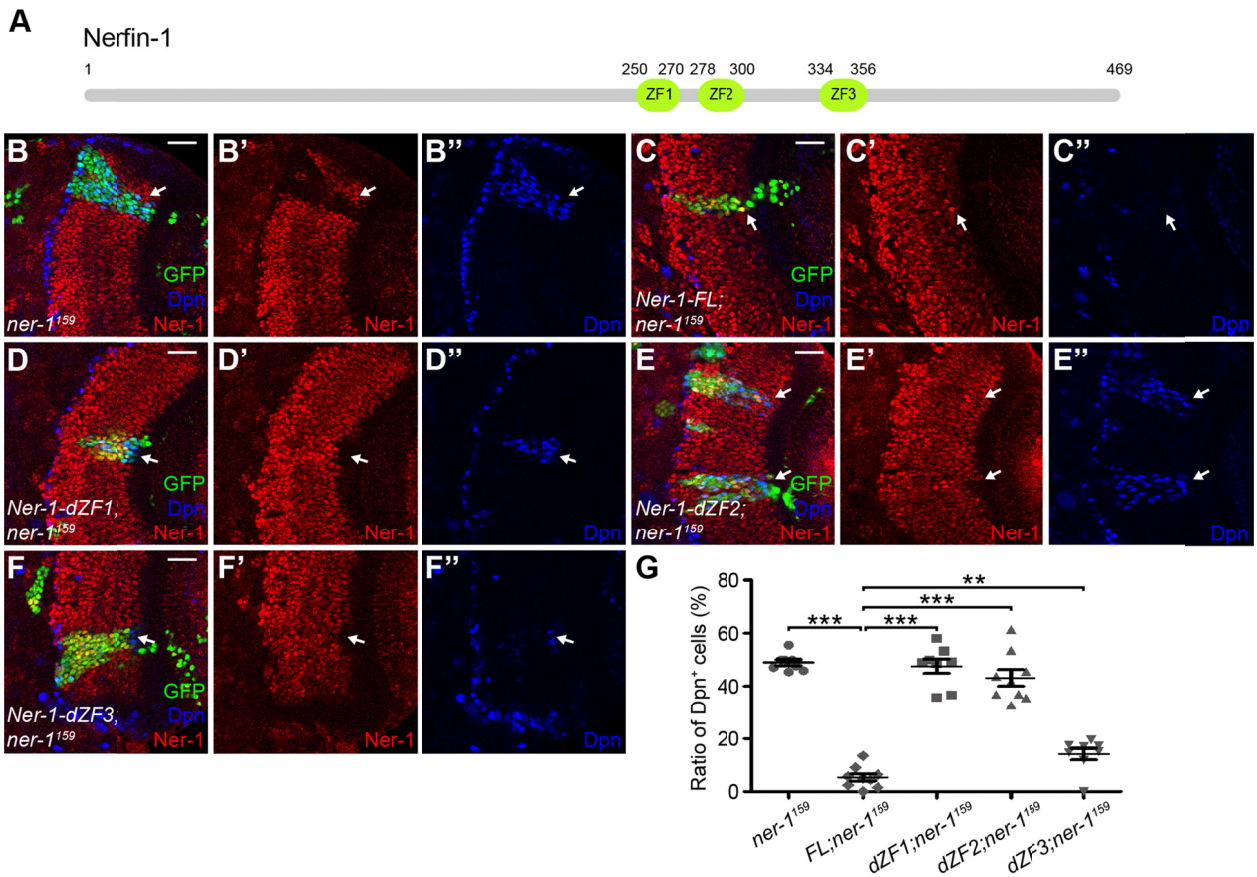

Figure. S3 All of the three zinc fingers contribute to the function of Nerfin-1.

(A) Schematic representation of Nerfin-1. Three zinc finger domains are shown. (B-F'') Misexpression of Nerfin-1 full length mostly rescues the dedifferentiation, while Nerfin-1 truncations do not. All transgenic Nerfin-1 proteins are expressed normally (C',D',E',F'). Arrows mark the clones. (G) Quantification of the ratio of Dpn^{+} cells in clones from (B,C,D,E,F). n=8,9,8,9,8, respectively. Mean±SEM; ** $p<0.01$; *** $p<0.001$. Scale bars represent 20 μm.

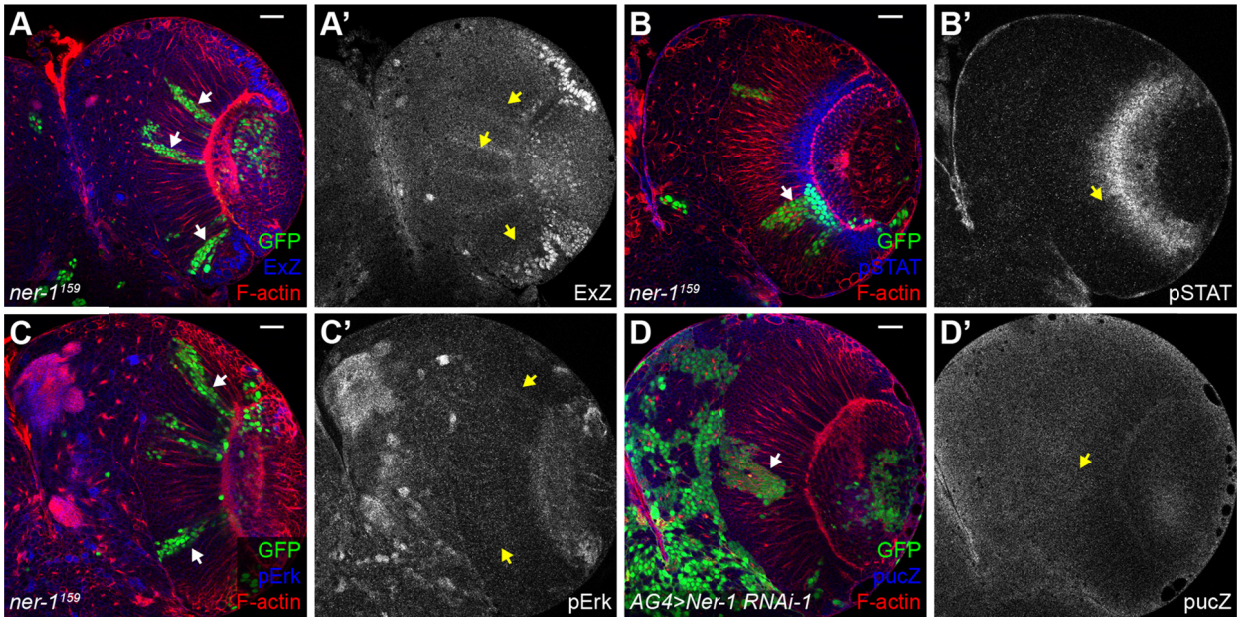

Figure. S4 Nerfin-1 loss-of-function does not affect the activity of Hippo, JAK/STAT, EGFR or JNK signaling pathways.

(A-D') Expression level of Ex-lacZ (A,A'), pSTAT (B,B'), pErk (C,C') or puc-lacZ (D,D') is used to represent the activity of Hippo, JAK/STAT, EGFR and JNK signaling respectively. None of them show obvious change when Nerfin-1 is depleted. Arrows mark the clones. Scale bars represent 20 μm.

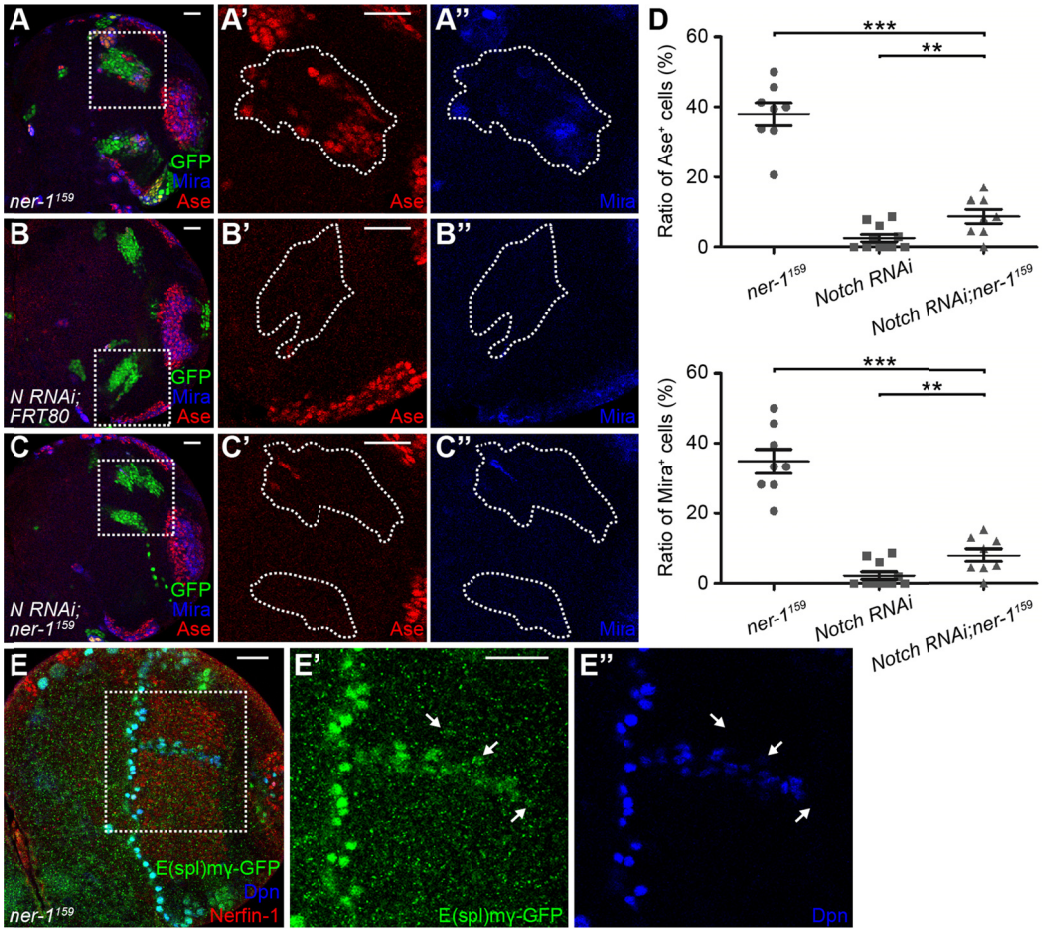

Figure. S5 Notch pathway hyperactivation is a cause rather than a consequence of dedifferentiation.

(A-C'') Notch knockdown mostly inhibits the ectopic expression of Mira and Ase caused by Nerfin-1 loss. Magnification of boxed regions in (A,B,C) is shown in (A',A'',B',B'',C',C'') respectively with clones outlined. (D) Quantification of the ratio of Ase^{+} or $Mira^{+}$ cells in clones from (A,B,C). For both Ase and Mira groups, n=8,11,8, respectively. Mean±SEM; ** $p<0.01$; *** $p<0.001$. (E-E'') Representative *nerfin-1*^{159} clones showing E(spl)m γ -GFP and Dpn staining. Magnification of boxed region in (E) is shown in (E',E''). Clone is marked by loss of Nerfin-1. Arrows mark the E(spl)m γ -GFP^{+}/Dpn^{-}(or weak) cells. Scale bars represent 20 μm.

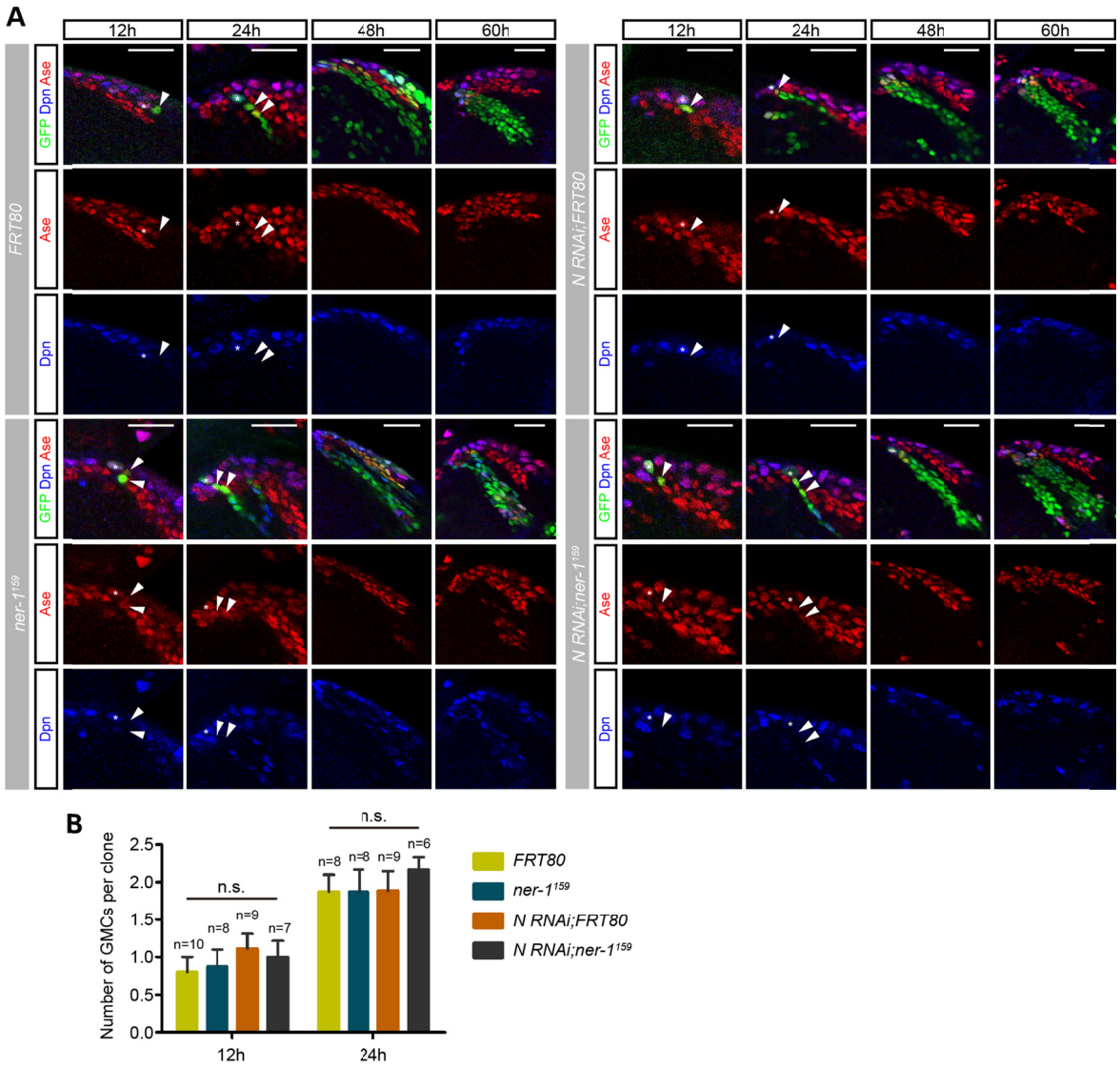

Figure. S6 Notch knockdown doesn't affect NB lineage generation, but blocks the dedifferentiation caused by Nerfin-1 absence.

(A) Time-course experiment showing Dpn and Ase staining. Representative clones of NB lineages labeled by GFP are shown. NB and GMC are marked by asterisk and arrowhead. Scale bars represent 20 μm. (B) Quantification of the number of GMCs in clones from (A). Mean±SEM; n.s. no significant.

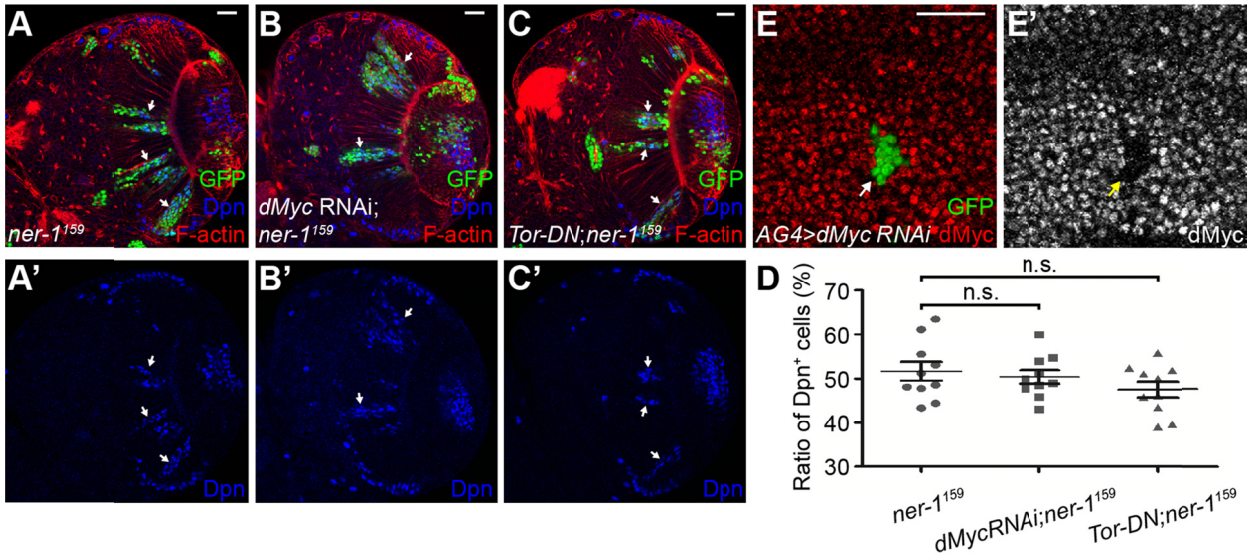

Figure. S7 Nerfin-1 doesn't function through dMyc or Tor in the optic lobe.

(A-C') Neither knockdown of dMyc nor misexpression of Tor dominant negative form can rescue the dedifferentiation in *nerfin-1*^{159} clones. Arrows mark the clones. (D) Quantification of the ratio of Dpn^{+} cells in clones from (A,B,C). n=10 for each. Mean±SEM; n.s. no significant. (E-E') Efficiency of dMyc RNAi is confirmed in larval wing discs. Arrows mark the clone. Scale bars represent 20 μm.

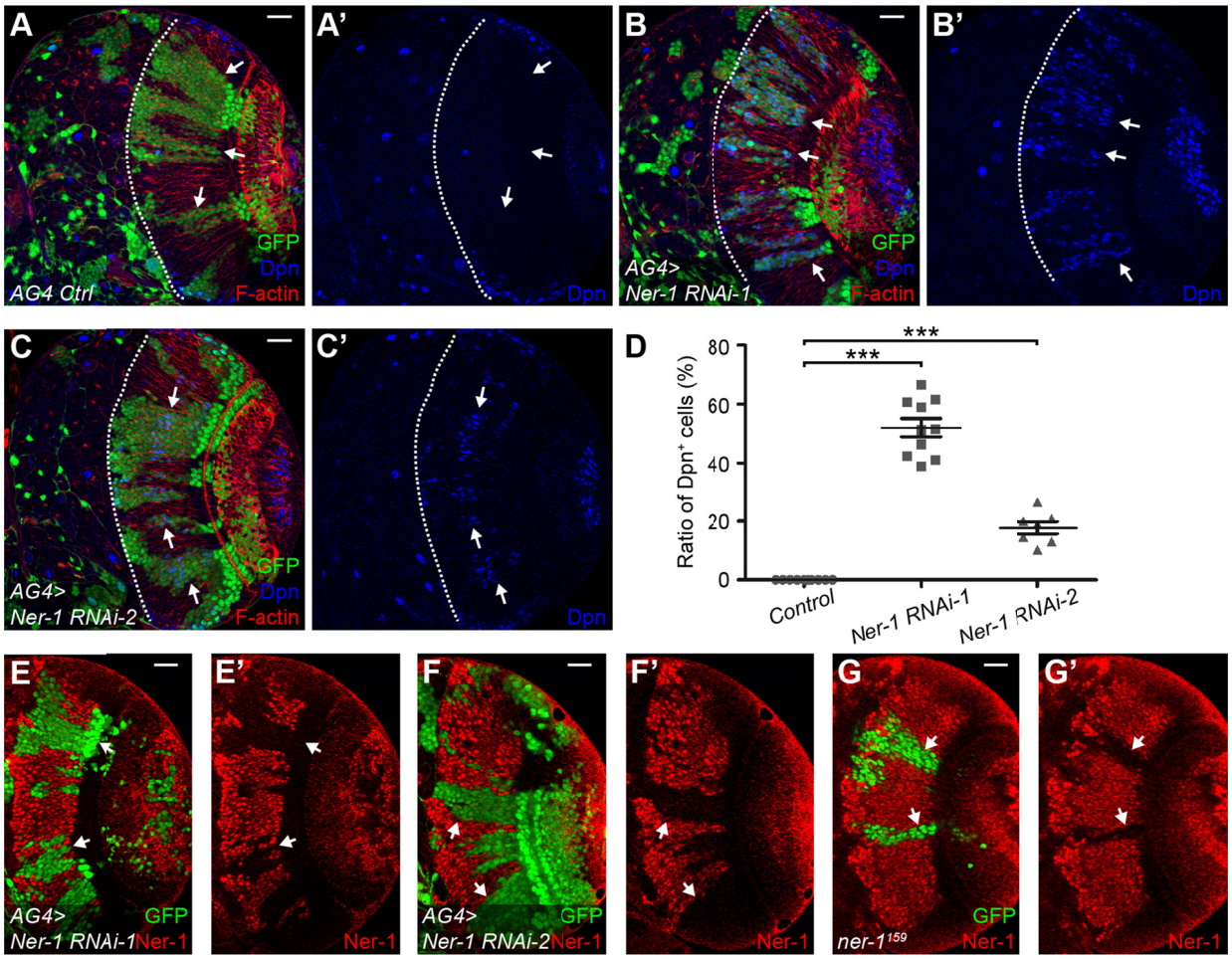

Figure. S1. Nerfin-1 knockdown results in ectopic NBs in medulla cortex.

(A-C') Knockdown of Nerfin-1 induces ectopic Dpn^{+} cells. Arrows show the clones. Dashed lines represent the boundary between central brain and the optic lobe. (D) Quantification of the ratio of Dpn^{+} cells in clones from A-C (n=10,10,7, respectively). Data are mean±s.e.m.; ***P<0.001. (E-G') Confirmation of the efficiency of Nerfin-1 RNAi lines (E-F') or *nerfin-1*^{159} fly (G,G'). Arrows show the clones. Clones are all labeled by GFP. Scale bars: 20 μm.

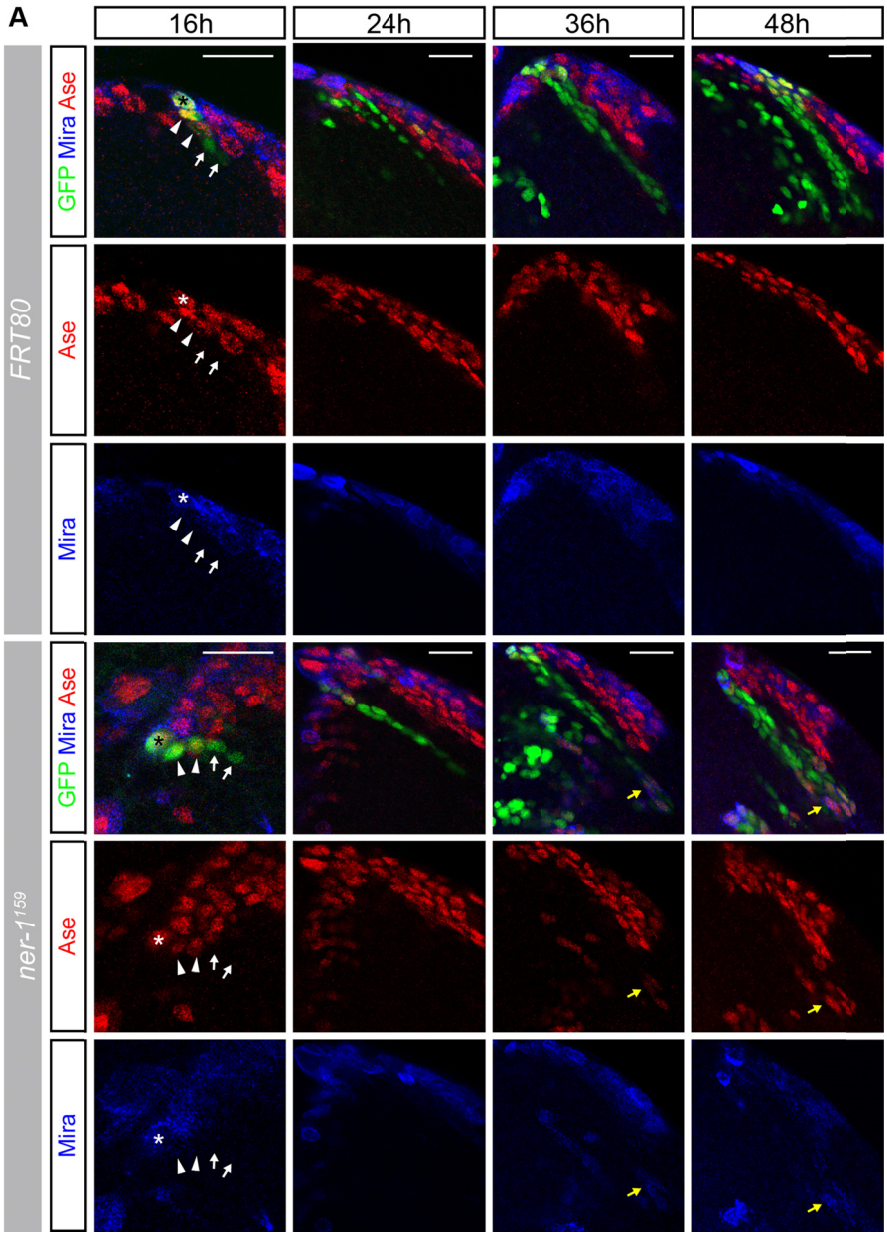

Figure. S2. Nerfin-1 loss leads to ectopic expression of Mira and Ase.

(A) Time-course experiment showing Mira and Ase staining. Representative NB lineages labeled by GFP are shown. Asterisk, arrowhead and arrow indicate NB, GMC and neuron, respectively, in clones of 16 h old. Yellow arrows show ectopic expression of Mira and Ase in *nerfin-1*^{159} clones. Scale bars: 20 μm.

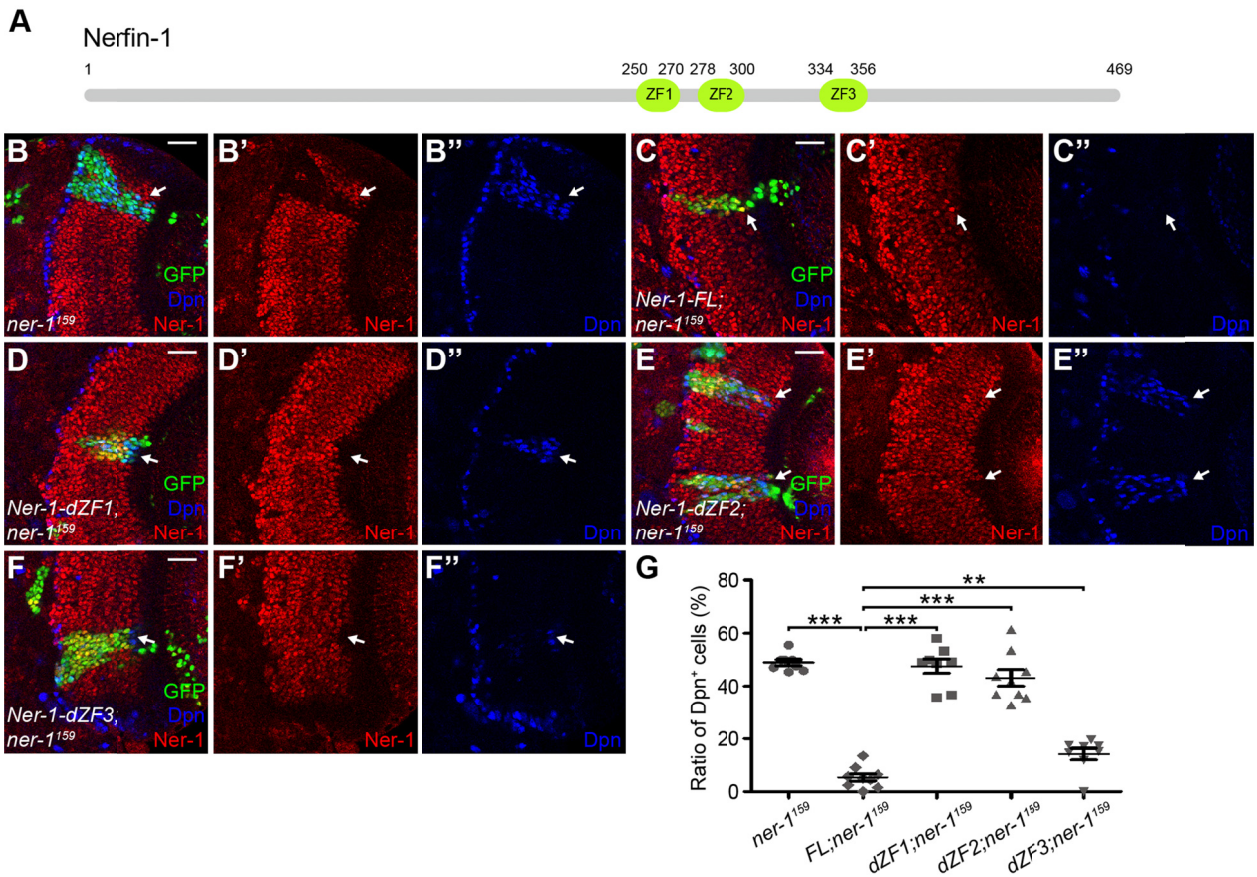

Figure. S3. All three zinc fingers contribute to Nerfin-1 function.

(A) Schematic representation of Nerfin-1. Three zinc finger domains are shown. (B-F'') Misexpression of Nerfin-1 full-length mostly rescues the dedifferentiation, while Nerfin-1 truncations do not. All transgenic Nerfin-1 proteins are expressed normally (C',D',E',F'). Arrows indicate the clones. (G) Quantification of the ratio of Dpn^+ cells in clones from B-F (n=8,9,8,9,8, respectively). Data are mean±s.e.m.; $^{**}P<0.01$; $^{***}P<0.001$. Scale bars: 20 μm.

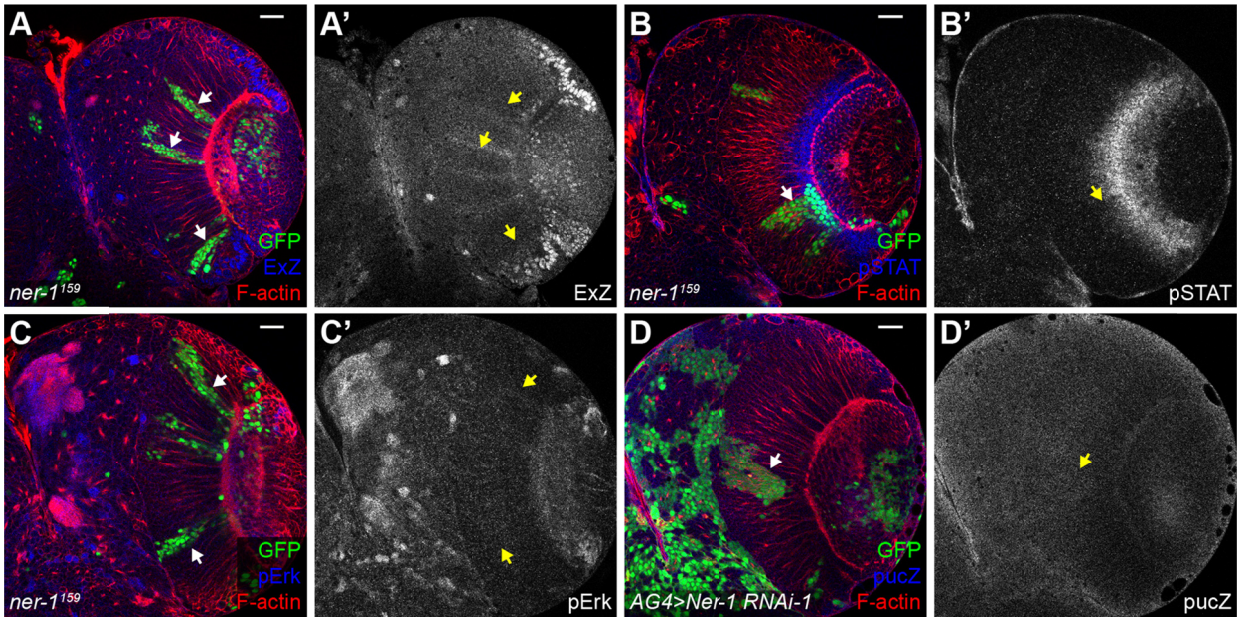

Figure. S4. Nerfin-1 loss-of-function does not affect the activity of Hippo, JAK/STAT, EGFR or JNK signaling pathways.

(A-D') Expression level of Ex-lacZ (A,A'), pSTAT (B,B'), pErk (C,C') or puc-lacZ (D,D') is used to represent the activity of Hippo, JAK/STAT, EGFR and JNK signaling, respectively. None of them is obviously altered when Nerfin-1 is depleted. Arrows show the clones. Scale bars: 20 μm.

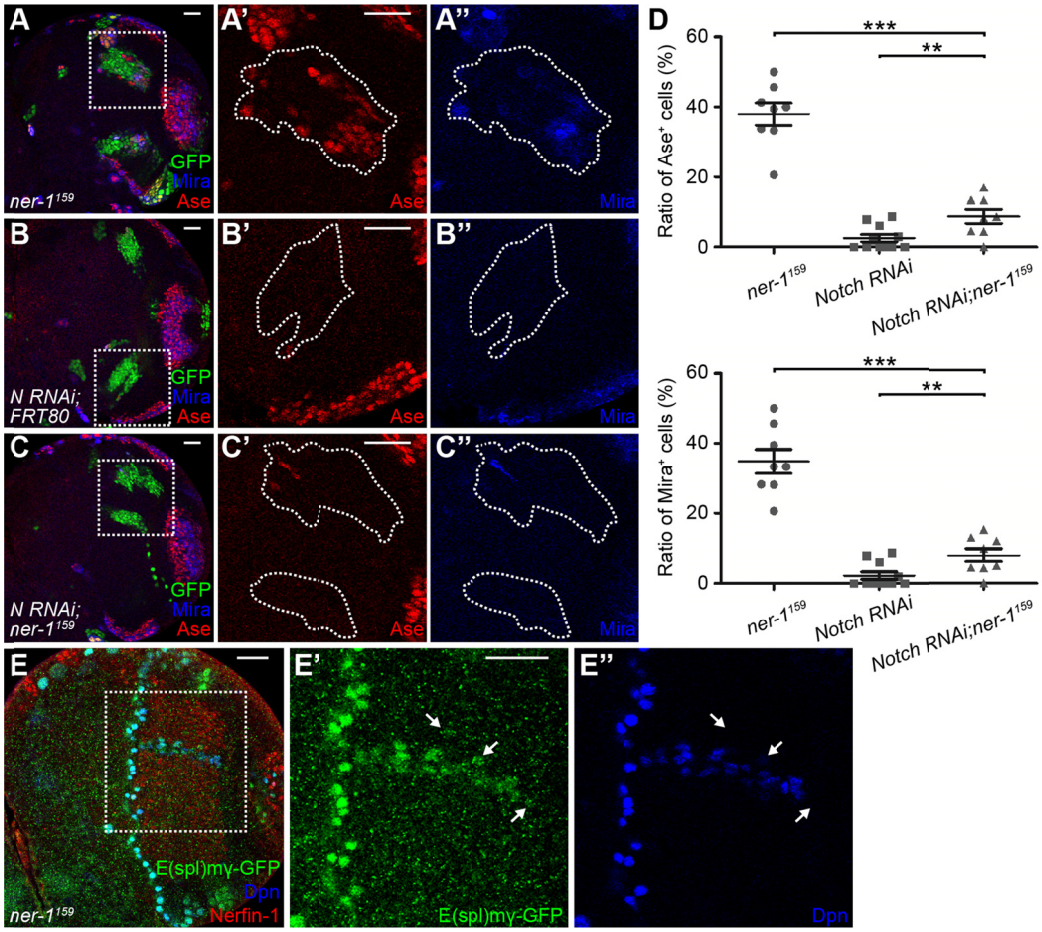

Figure. S5. Notch pathway hyperactivation is a cause rather than a consequence of dedifferentiation.

(A-C'') Notch knockdown mostly inhibits the ectopic expression of Mira and Ase caused by Nerfin-1 loss. Magnification of boxed regions in A-C is shown in A'-C'', respectively, with clones outlined. (D) Quantification of the ratio of Ase^{+} or $Mira^{+}$ cells in clones from A-C (n=8,11,8, respectively). Data are mean±s.e.m.; $^{**}P<0.01$; $^{***}P<0.001$. (E-E'') Representative *nerfin-1*^{159} clones showing E(spl)mγ-GFP and Dpn staining. Magnification of boxed region in E is shown in E' and E''. Clones are labeled by loss of Nerfin-1. Arrows indicate the E(spl)mγ-GFP^{+}/Dpn^{-}(or weak) cells. Scale bars: 20 μm.

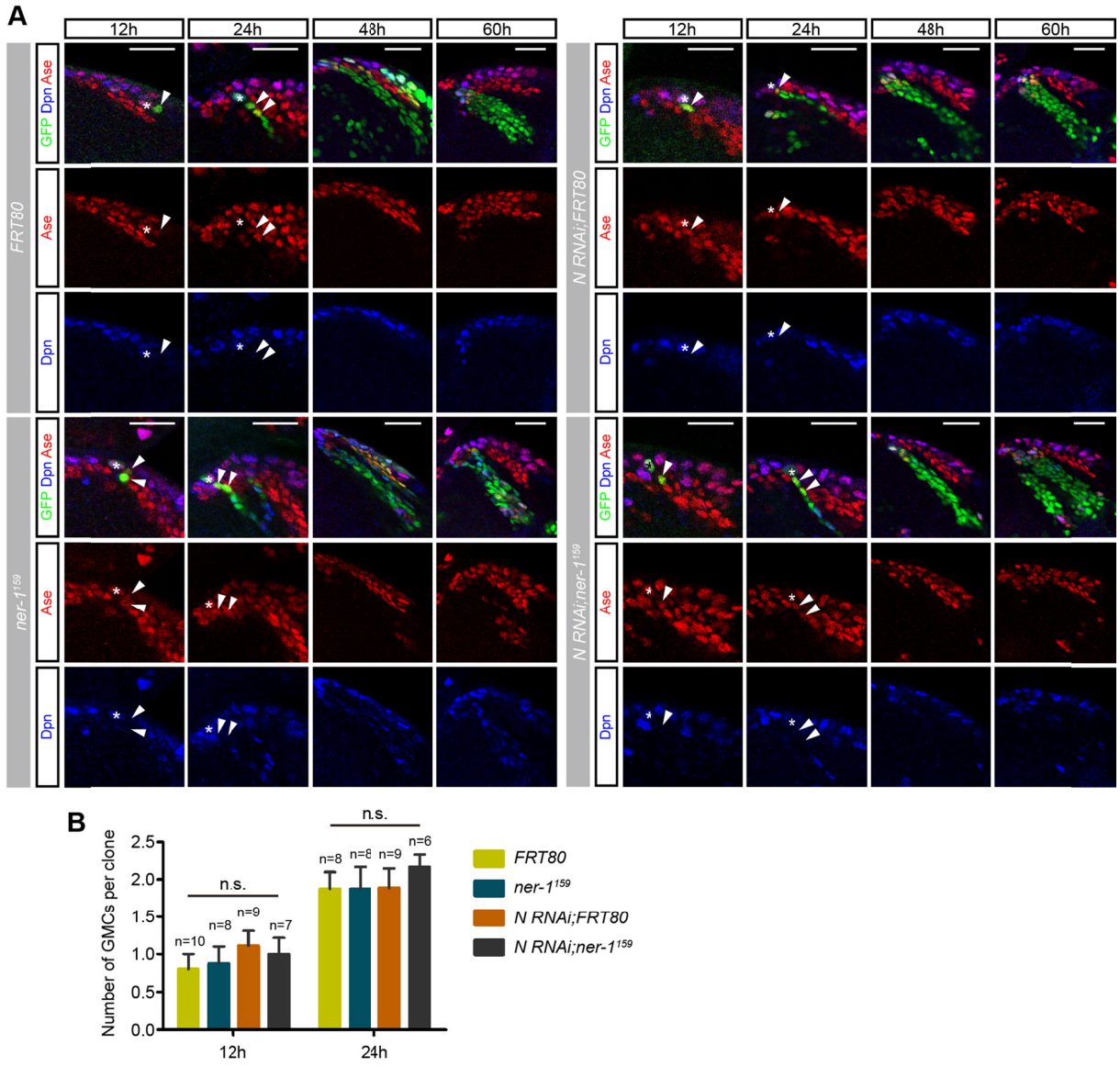

Figure. S6. Notch knockdown doesn't affect NB lineage generation, but blocks the dedifferentiation caused by Nerfin-1 absence.

(A) Time-course experiment showing Dpn and Ase staining. Representative NB lineages labeled by GFP are shown. NB and GMC are indicated by asterisk and arrowhead, respectively. Scale bars: 20 μm. (B) Quantification of the number of GMCs in clones from A. Data are mean± s.e.m.; n.s., no significant.

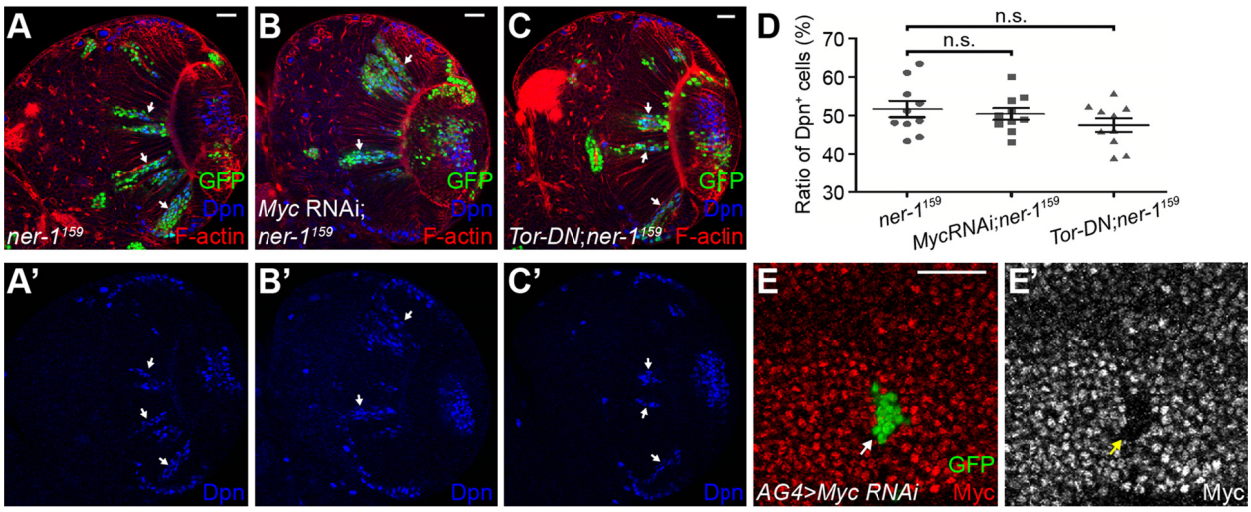

Figure. S7. Nerfin-1 doesn't function through Myc or Tor in the optic lobe.

(A-C') Neither knockdown of Myc nor misexpression of Tor dominant negative form can rescue the dedifferentiation in *nerfin-1*^{159} clones. Arrows show the clones. (D) Quantification of the ratio of Dpn^{+} cells in clones from A-C (n=10 for each). Data are mean±s.e.m.; n.s., no significant. (E-E') Efficiency of Myc RNAi is confirmed in larval wing discs. Arrows show the clones. Scale bars: 20 μm.